

LAGRANGIAN FILLINGS IN A-TYPE AND THEIR KALMAN LOOP ORBITS

JAMES HUGHES

ABSTRACT. We continue the study of exact Lagrangian fillings of Legendrian $(2, n)$ torus links, as first initiated by Ekholm-Honda-Kalman and Pan. Our main result proves that for a decomposable exact Lagrangian filling described through a pinching sequence, there exists a unique weave filling in the same Hamiltonian isotopy class. As an application of this result we describe the orbital structure of the Kalman loop and give a combinatorial criteria to determine the orbit size of a filling. We first give a Floer-theoretic proof of the orbital structure, where an identity studied by Euler in the context of continued fractions makes a surprise appearance. This is followed by an alternative geometric proof of the orbital structure, obtained as a corollary of the main result. We conclude by giving a purely combinatorial description of the Kalman loop action on the fillings discussed above in terms of edge flips of triangulations.

1. INTRODUCTION

Legendrian links and their exact Lagrangian fillings are objects of interest in contact and symplectic topology [?, ?, ?, EN19]. Within the last decade, parallel developments in the construction of fillings [CZ21, EHK16] and the application of both Floer-theoretic [CN21, GSW20, Pan17] and microlocal-sheaf-theoretic [CG20, STZ17, TZ18] invariants have significantly advanced the classification of fillings. Broadly speaking, this manuscript aims to compare the two primary methods of constructing fillings, [TZ18] and [EHK16], in the well-studied case of Legendrian $(2, n)$ torus links in the standard contact 3-sphere. In addition to a contact geometric approach, we discuss insights into properties of the augmentation variety associated to this class of Legendrian links afforded by this comparison.

If we denote by σ the Artin generator of the braid group on two strands, then the family of maximal-tb Legendrian $(2, n)$ torus links is defined in the front projection as the rainbow closure of the positive braid σ^n , as depicted in Figure 1 (left). Smoothly, the $(2, n)$ torus link is also described as the link of the complex A_{n-1} -singularity $f(x, y) = x^n + y^2$. In general, the max-tb representatives of algebraic links are Legendrian simple [Cas21, Proposition 2.2], hence we will also refer to the max-tb Legendrian $(2, n)$ torus link as an A -type Legendrian link, denoted $\lambda(A_{n-1}) \subseteq (\mathbb{S}^3, \xi_{st})$. The Lagrangian fillings that we will consider in this manuscript are all exact and embedded in the standard symplectic 4-ball $(\mathbb{D}^4, \lambda_{st})$, whose boundary is the standard contact 3-sphere (\mathbb{S}^3, ξ_{st}) .

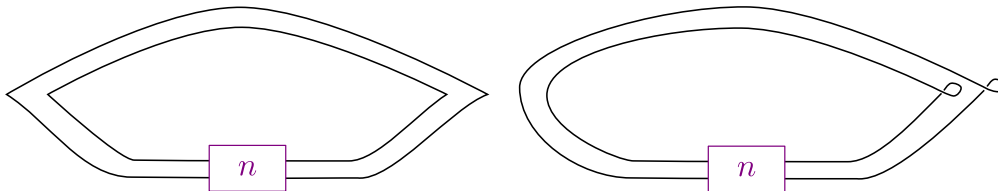


FIGURE 1. The front projection (left) and Ng resolution [Ng03] (right) of the Legendrian torus link $T(2, n) = \lambda(A_{n-1})$, equivalently described as the rainbow closure of the braid σ^n . The n appearing in each of the diagrams represents n positive crossings.

2020 *Mathematics Subject Classification.* 53D12, 53D35; 53D10, 57K10, 57K33.

Key words and phrases. Lagrangian fillings, Legendrian knots, Triangulations, Euler's continuants, Euler's identity.

1.1. Main Results. This article has two primary independent contributions, one algebraic and the other geometric.

First, we begin by sketching the two constructions of Lagrangian fillings needed to state our geometric result. The first construction of Lagrangian fillings of $\lambda(A_{n-1})$ was given by Ekholm-Honda-Kalman in [EHK16]. In their construction, a filling L_σ is labeled by a permutation σ in S_n , specifying an order of resolving the n crossings of $\lambda(A_{n-1})$. The elementary cobordism used to resolve those crossings will be referred to as a pinching cobordism. The Lagrangian fillings constructed in [EHK16] were then separated into distinct Hamiltonian isotopy classes and indexed to 312-avoiding permutations by Yu Pan in [Pan17], using Floer-theoretic methods. Pan's result shows that there are at least a Catalan number $C_n = \frac{1}{n+1} \binom{2n}{n}$ of Lagrangian fillings of $\lambda(A_{n-1})$ obtained via pinching cobordisms. These fillings will be referred to as pinching sequence fillings and the set of (Hamiltonian isotopy classes of) fillings as \mathcal{P}_n .

In [TZ18], Treumann and Zaslow gave an alternative construction of a Catalan number of Lagrangian fillings of $\lambda(A_{n-1})$ and distinguished them using microlocal sheaf theory. These Lagrangian fillings are represented by planar trivalent graphs and indexed by the triangulated $(n+2)$ -gons dual to such graphs. Given a triangulation \mathcal{T} of a regular $(n+2)$ -gon, we will denote the filling represented by the 2-graph dual to \mathcal{T} by $L_{\mathcal{T}}$. Adopting the terminology of [CZ21], we refer to $L_{\mathcal{T}}$ as a weave filling and denote the set of (Hamiltonian isotopy classes of) weave fillings of $\lambda(A_{n-1})$ as \mathcal{W}_n . We also refer to the elementary cobordism in this construction as a D_4^- cobordism after Arnold's classification of wavefront singularities [Ad90]. In Section 2 we give an explicit construction of both a pinching cobordism and a D_4^- cobordism. In Section 4, we describe a Hamiltonian isotopy between the local model describing an elementary pinching cobordism and the local model describing the D_4^- cobordism. This equivalence is then used to prove our first main result:

Theorem 1.1. *For any exact Lagrangian filling of $\lambda(A_{n-1})$ constructed via a sequence of pinching cobordisms, there is unique a Hamiltonian isotopic weave filling. That is, given a 312-avoiding permutation σ , the filling L_σ is Hamiltonian isotopic to the filling $L_{\mathcal{T}}$ for a unique triangulation \mathcal{T} .*

An immediate consequence of Theorem 1.1 is that the two sets of a Catalan number of (Hamiltonian isotopy classes of) exact Lagrangian fillings \mathcal{W}_n and \mathcal{P}_n constructed in [TZ18] and [Pan17] coincide. This is in agreement with the conjectured ADE-classification of exact Lagrangian fillings [Cas21, Conjecture 5.1] where $\lambda(A_{n-1})$ is conjectured to have exactly a Catalan number C_n of distinct fillings up to Hamiltonian isotopy.

Theorem 1.1 appears as a protagonist in another central narrative of our study, an exploration of the orbital structure of the Kalman loop action on Lagrangian fillings of $\lambda(A_{n-1})$. Introduced by the eponymous mathematician in [Kál05], the Kalman loop is a Legendrian isotopy that acts on the set of fillings of a torus link $T(m, n)$ by permuting the order in which crossings are resolved by elementary cobordism. For weave fillings, the Kalman loop action is readily understood by the combinatorics of the triangulation of the dual $(n+2)$ -gon under the action of rotation. Theorem 1.1 therefore allows us to geometrically deduce the orbital structure of the Kalman loop action on the set of pinching sequence fillings where it is otherwise more mysterious.

Second, independently, and preceding the discussion of our geometric result, we also give a Floer-theoretic proof of the orbital structure of the Kalman loop by examining its action on the augmentation variety $\text{Aug}(\lambda(A_{n-1}))$. The augmentation variety is a Floer-theoretic invariant associated to a Legendrian link. In [EHK16], it was shown that a filling of a Legendrian λ endowed with a choice of a local system can be interpreted geometrically as a point in the augmentation variety $\text{Aug}(\lambda)$. In this way, the augmentation variety can be thought of as a moduli space of fillings for a given

Legendrian. The Kalman loop induces an automorphism of the augmentation variety and we can study this automorphism to understand the orbital structure of the Kalman loop action on fillings.

In this setting we introduce our second protagonist, a set of regular functions $\Delta_{i,j}$ on $\text{Aug}(\lambda(A_{n-1}))$, which we show correspond to diagonals of a triangulated $(n+2)$ -gon. These regular functions admit an additional characterization as continuants, recursively defined polynomials studied by Euler in the context of continued fractions [Eul64]. This characterization leads to the appearance of a key supporting character, Euler's identity for continuants. Continuants naturally appear in the definition of the augmentation variety of $\lambda(A_{n-1})$ [CGGS20], and in Section 3 we show that the action of the Kalman loop is identical to Euler's continuant identity. In this sense, we may interpret the Kalman loop action on the augmentation variety as a Floer-theoretic manifestation of Euler's identity for continuants. Conversely, our geometric story may therefore be characterized as a somewhat convoluted proof of the continuant identity through contact geometry.

Paralleling the geometric story, we prove in Subsection 3.2 that the $\Delta_{i,j}$ give coordinate functions on the toric chart in $\text{Aug}(\lambda(A_{n-1}))$ induced by a pinching sequence filling. From this algebraic argument, we conclude that the orbital structure of the Kalman loop corresponds precisely to the orbits of triangulations under rotation. The main results of this story are summarized in the two-part theorem below.

Theorem 1.2. *The action of the Kalman loop on the set \mathcal{P}_n , the Catalan number of exact Lagrangian fillings of A -type satisfies:*

- (1) *The number of Kalman loop orbits of fillings of $\lambda(A_{n-1})$ is*

$$\frac{C_n}{n+2} + \frac{C_{(n)/2}}{2} + \frac{2C_{n/3}}{3}$$

where the terms with $C_{n/2}$ and $C_{n/3}$ appear if and only if the indices are integers.

- (2) *The action of the Kalman loop on the regular functions $\Delta_{i,j} \in \mathbb{C}[(\text{Aug}(\lambda(A_{n-1})))]$ is equivalent to Euler's identity for continuants, where $\text{Aug}(\lambda(A_{n-1}))$ is the augmentation variety of $\lambda(A_{n-1})$.*

Following both of our proofs of Theorem 1.2, we conclude our exploration of the Kalman loop with a discussion of its combinatorial properties. We first describe a method for determining the orbit size of a filling based solely on the associated 312-avoiding permutation.

Theorem 1.3. *There exists an algorithm of complexity $O(n^2)$ with input a 312-avoiding permutation σ in S_n for determining the orbit size of a pinching sequence filling L_σ under the Kalman loop action.*

See Subsection 5.1 for the algorithm. In addition, we give an entirely combinatorial description of the Kalman loop action in terms of 312-avoiding permutations as a sequence of edge flips of triangulations. The appearance of triangulated polygons and edge flips is perhaps best explained as the manifestation of the theory of cluster algebras lurking in the background. While cluster theory does not explicitly appear in any of our proofs, we highlight the connections where relevant. We refer the reader to [GSW20] for a more dedicated treatment of cluster structures on the augmentation variety.

Although we do not prove it here, we claim that the techniques of Theorem 1.1 generalize to the setting of rainbow closures of n -stranded braids. As a result, any Lagrangian filling constructed as a pinching sequence can be shown to be Hamiltonian isotopic to a weave filling. As a possible application of the above claim, we might hope to describe the orbital structure of fillings of $\lambda(D_n)$ under the action of analogous Legendrian loops. In this context, the combinatorics of tagged triangulations are the D -type analog of the triangulations appearing in A -type. However, there is

currently no known bijection between tagged triangulations and D -type weaves, as constructed in [Hug21].

Organization. In Section 2, we cover the necessary preliminaries, including the constructions of exact Lagrangian fillings, the Legendrian contact differential graded algebra, the Kalman loop, and related combinatorics. Section 3 contains the Floer-theoretic proof of Theorem 1.2, featuring Euler’s continuant identity. In Section 4, we prove Theorem 1.1, from which we obtain our geometric proof of Theorem 1.2 as a corollary. Finally, Section 5 presents the orbit size algorithm of Theorem 1.2, and we conclude with a combinatorial description of the Kalman loop action on these permutations.

Acknowledgements. Many thanks to Roger Casals for his help and encouragement throughout. Thanks also to Lenny Ng for the original question on Kalman loop orbits that motivated this project.

2. PRELIMINARIES ON LEGENDRIAN LINKS AND THEIR INVARIANTS

2.1. Legendrian links and Lagrangian fillings. We begin with the necessary preliminaries from contact and symplectic topology. The standard contact structure ξ_{st} in \mathbb{R}^3 is the 2-plane field given as the kernel of the 1-form $\alpha = dz - ydx$. A link $\lambda \subseteq (\mathbb{R}^3, \xi_{st})$ is Legendrian if λ is always tangent to ξ_{st} . As λ can be assumed to avoid a point, we can equivalently consider Legendrians λ contained in the contact 3-sphere (\mathbb{S}^3, ξ_{st}) [Gei08, Section 3.2].

The symplectization of contact \mathbb{R}^3 is the symplectic manifold $(\mathbb{R}^3 \times \mathbb{R}_t, d(e^t\alpha))$. Given two Legendrian links λ_- and λ_+ , an exact Lagrangian cobordism $L \subseteq (\mathbb{R}^3 \times \mathbb{R}_t, d(e^t\alpha))$ from λ_- to λ_+ is a cobordism Σ such that there exists some $T > 0$ satisfying the following:

- (1) $d(e^t\alpha)|_{\Sigma} = 0$
- (2) $\Sigma \cap ((-\infty, T] \times \mathbb{R}^3) = (-\infty, T] \times \lambda_-$
- (3) $\Sigma \cap ([T, \infty) \times \mathbb{R}^3) = [T, \infty) \times \lambda_+$
- (4) $e^t\alpha|_{\Sigma} = df$ for some function f on Σ .

An exact Lagrangian filling of the Legendrian link $\lambda \subseteq (\mathbb{R}^3, \xi_{st})$ is an exact Lagrangian cobordism L from \emptyset to λ that is embedded in the symplectization $\mathbb{R}^3 \times \mathbb{R}$. Equivalently, we consider L to be embedded in the symplectic 4-ball with boundary ∂L contained in the contact 3-sphere (\mathbb{S}^3, ξ_{st}) [AdG01, Section 6.2]. In A -type, our fillings will be constructed as a series of saddle cobordisms and minimum cobordisms.

We now describe the precise topological construction of the elementary cobordisms defining pinching sequence and weave fillings. For a pinching cobordism, consider the neighborhood of a crossing in the Lagrangian projection. If this crossing is contractible, i.e., the distance between the two strands can be made arbitrarily small, then attaching a 1-handle yields an exact Lagrangian cobordism in the symplectization $(\mathbb{R}^3 \times \mathbb{R}_t, d(e^t(dz - ydx)))$ [EHK16]. If λ is the rainbow closure of a positive braid, as is the case for $\lambda(A_{n-1})$, then every crossing is contractible [CN21]. See Figure 2 for a local model depicting this cobordism as a 0-resolution in the Lagrangian projection, $\Pi : (\mathbb{R}^3, \xi_{st}) \rightarrow \mathbb{R}^2, \Pi(x, y, z) = (x, y)$.

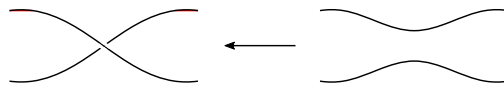


FIGURE 2. A local model of a pinching cobordism as a 0-resolution of a contractible crossing in the Lagrangian projection. The direction of the arrow indicates a cobordism from the concave end to the convex end.

Let us consider $\lambda \subseteq (\mathbb{R}^3, \xi_{st})$ and its front projection $\pi(\lambda)$, where $\pi : (\mathbb{R}^3, \xi_{st}) \rightarrow \mathbb{R}^2$, $\pi(x, y, z) = (x, z)$. In order to apply the pinching cobordism to a Legendrian $\lambda \subseteq (\mathbb{R}^3, \xi_{st})$, we use the Ng resolution. This is a Legendrian isotopy λ_t such that $\lambda_0 = \lambda$ and the Lagrangian projection $\Pi(\lambda_1)$ can be obtained from the front projection $\pi(\lambda_1)$ by smoothing all left cusps and replacing all right cusps with small loops [Ng03]. A pinching cobordism in the front projection of the link $\lambda(A_{n-1})$ is then given by first taking the Ng resolution of $\lambda(A_{n-1})$ – depicted in Figure 1 (right) – resolving a crossing in the Lagrangian projection as specified above, and then undoing the Ng resolution.

Given that $\lambda(A_{n-1})$ has n crossings, a pinching sequence filling can be characterized by a permutation σ in S_n . Such a permutation specifies an order in which to apply these elementary cobordisms to the n contractible (degree 0) crossings in the Ng resolution of $\lambda(A_{n-1})$. Given a permutation σ of the form $\dots i k \dots j$ for $i > k > j$, the permutation $\sigma' = \dots k i \dots j$ obtained by interchanging i and k gives an order of pinching crossings that yields the same Floer-theoretic invariant¹ [Pan17]. A permutation σ such that any triple of letters i, j, k appearing in order in σ does not satisfy the inequality $i > k > j$ is referred to as a 312-avoiding permutation. Distinct 312-avoiding permutations yield distinct Hamiltonian isotopy invariants of exact Lagrangian fillings, i.e. restricting the indexing set from S_n to 312-avoiding permutations yields the existence of at least a Catalan number of fillings of $\lambda(A_{n-1})$ up to Hamiltonian isotopy [Pan17].

For a D_4^- cobordism, consider the Legendrian in J^1S^1 with front projection given as the (-1)-framed closure of the braid $\sigma_1^n \Delta^2 = \sigma_1^{n+2}$. A contact embedding of $i : S^1 \rightarrow \mathbb{R}^3$ yields an embedding of J^1S^1 into a small open neighborhood of $i(S^1)$. In particular, a Legendrian link in J^1S^1 is sent to the standard satellite of $i(S^1)$ in \mathbb{R}^3 . For two-stranded braids, the standard satellite of the (-1)-framed closure of σ_1^{n+2} is the rainbow closure of σ_1^n , so we recover our original description of $\lambda(A_{n-1})$.

We can take the embedding i to be the restriction of a contact embedding of a disk D^2 into (\mathbb{R}^5, ξ_{st}) to its boundary ∂D^2 . The embedding of J^1S^1 into an open neighborhood of $i(S^1)$ is then a direct consequence of an embedding of $(J^1D^2, \xi_{st}) = (T^*D^2 \times \mathbb{R}_z, dz - \lambda_{st})$ into an open neighborhood of $i(D^2)$ where λ_{st} is the standard Liouville form on T^*D^2 . To define an exact Lagrangian cobordism, we first describe a Legendrian cobordism in J^1D^2 . Taking the Lagrangian projection of this cobordism then yields an exact Lagrangian in symplectic \mathbb{R}^4 . A slicing of the Legendrian cobordism is depicted in Figure 3 and is described as follows. Near a contractible Reeb chord trapped between two crossings, we apply a Reidemeister I move and Legendrian isotopy to shrink the Reeb chord. We then add a 1-handle to remove this Reeb chord and apply another pair of Reidemeister I moves to simplify to a diagram with one fewer crossings than we started with. The graph of this process forms a surface in $J^1[a, b]$ and yields an exact Lagrangian cobordism in symplectic \mathbb{R}^4 by taking the Lagrangian projection of its embedding in contact \mathbb{R}^5 . The front of this graph yields a D_4^- singularity in $D^2 \times \mathbb{R}$, hence the name.

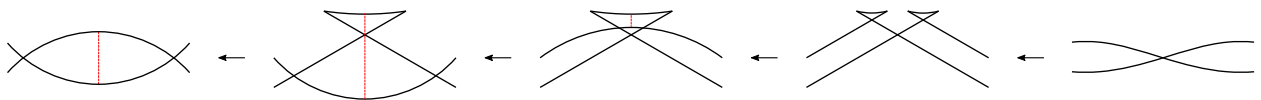


FIGURE 3. A local model of a D_4^- cobordism in the front projection. The Reeb chord is depicted as a dashed red line. We first apply a Reidemeister I move before removing the Reeb chord and applying two more Reidemeister I moves to arrive at a diagram with a single crossing. By convention, we will identify the remaining crossing with the leftmost crossing of the original pair.

¹The two fillings corresponding to σ and σ' yield identical augmentations ϵ_σ and $\epsilon_{\sigma'}$ of the DGA $\mathcal{A}(\lambda(A_{n-1}))$. This is because the presence of the crossing labeled j prevents the existence of any holomorphic strip with positive punctures occurring at both crossings i and k . Therefore, resolving crossing k (resp. i) has no effect on the generator z_i (resp. z_k) in the DGA $\mathcal{A}(\lambda(A_{n-1}))$.

The set of fillings constructed with the D_4^- cobordism in [TZ18] is encoded by planar trivalent graphs. We refer to such a graph as a 2-graph and the Legendrian surface it represents as a Legendrian weave, following the terminology of [CZ21]. Given a 2-graph Γ , the Legendrian weave $\Lambda(\Gamma)$ is described topologically as the double branched cover over \mathbb{D}^2 , simply branched at the trivalent vertices of Γ . To ensure that the Lagrangian projection of the weave $\Lambda(\Gamma)$ yields an embedded surface in symplectic \mathbb{R}^4 , we require that $\Lambda(\Gamma)$ admits no Reeb chords. This occurs if and only if the trivalent graph Γ has no internal faces. Figure 4 (left) depicts an example of a 2-graph and its dual $(n+2)$ -gon representing an embedded filling of $\lambda(A_{n-1})$.

In order to prove Theorem 1.1 we will require a convention for relating trivalent vertices of a 2-graph to crossings in the Ng resolution. The vertical weave construction given originally in [CGGS20] allows us to unambiguously associate a trivalent vertex in the weave to the 0-resolution of a specific crossing in a pinching sequence filling by specifying a convention for breaking the symmetry of a 2-graph inscribed in a triangulated $(n+2)$ -gon.

Given a 2-graph Γ inscribed in a dual triangulation of the $(n+2)$ -gon, we construct a vertical weave by vertically orienting all of the edges of Γ intersecting the boundary of the $(n+2)$ -gon at the top of the page and choosing a convention for labeling. In this manuscript, we will fix the convention of labeling boundary edges by the number of the vertex most immediately counterclockwise. The boundary edges at top of the vertical weave are then labeled $n+2, 1, \dots, n+1$. With this choice of convention, the edge exiting a trivalent vertex when traversing the weave from top to bottom will inherit the label of the edge entering from the left. See Figure 4 for an example in the case $n=6$. Note that this choice differs from the convention in [CGGS20], as the choice of labeling given there corresponds to resolving the leftmost crossing of the pair in the D_4^- cobordism.

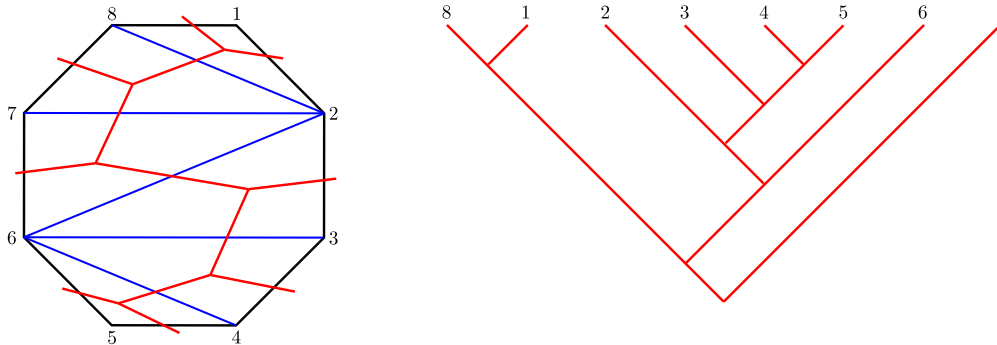


FIGURE 4. A pair of 2-graphs representing the same weave filling of $\lambda(A_5)$. On the left, the 2-graph Γ is inscribed in its dual triangulation of the octagon, while the corresponding vertical weave is depicted on the right. The edges of the vertical 2-graph are labeled by the nearest counterclockwise label of the dual triangulation and each trivalent vertex corresponds to a D_4^- cobordism that has the effect of resolving the rightmost crossing of the pair in the Ng resolution of the front projection. The bottom edge of a trivalent vertex therefore retains the label of the strand on the left.

It is claimed without proof in [Pan17] that, in addition to yielding the same Floer-theoretic invariant, there is a Hamiltonian isotopy between pinching sequence fillings represented by permutations $\sigma = \dots ik \dots j \dots$ and $\sigma' = \dots ki \dots j \dots$ in S_n . This claim implies that a 312-avoiding permutation represents a unique equivalence class of filling up to Hamiltonian isotopy. The claim follows from Theorem 1.1 and the lemma below

Lemma 2.1. *Let i, j , and k be vertex labels of a vertical 2-graph Γ with $i < j < k$ and j appearing below both i and k . The planar isotopy between Γ and the 2-graph Γ' obtained by exchanging the*

heights of i and k lifts to a compactly supported Hamiltonian isotopy of the fillings L_Γ and L'_Γ fixing the boundary.

Proof. By construction, the planar isotopy between Γ and Γ' lifts to a Legendrian isotopy between the weaves $\Lambda(\Gamma)$ and $\Lambda(\Gamma')$ in contact \mathbb{R}^5 . Note that this planar isotopy can be taken to be the identity at the boundary $\partial\Lambda(\Gamma)$. Considering the Lagrangian projection of this sequence of weaves yields a compactly supported exact Lagrangian isotopy between the Lagrangian fillings L_Γ and L'_Γ . By [FOOO09], this implies the existence of a compactly supported Hamiltonian isotopy between the two fillings. □

By Theorem 1.1, the exact Lagrangian isotopy of the weave filling extends to pinching sequence fillings. Thus, our result implies that there are exactly a Catalan number C_n of pinching sequence fillings² of $\lambda(A_{n-1})$ up to Hamiltonian isotopy.

2.2. The Legendrian contact DGA and its augmentations. For any Legendrian link λ , the Legendrian contact differential graded algebra (DGA) $\mathcal{A}(\lambda)$ is a powerful Floer-theoretic invariant of λ [Che02]. For a knot λ , the Legendrian contact DGA is freely generated over either \mathbb{Z}_2 or \mathbb{Z} by the Reeb chords of $\lambda \subseteq (\mathbb{R}^3, \xi_{st})$. The grading for a Reeb chord generator of $\mathcal{A}(\lambda)$ is roughly defined by the number of counterclockwise revolutions that a tangent vector makes while traversing along a capping path between the two endpoints of the Reeb chord [EN19]. In the case of $\lambda(A_{n-1})$, every Reeb chord that corresponds to a crossing of the braid σ^n in the Ng resolution has degree zero while the remaining two Reeb chords at the right of the diagram have degree one. With an appropriate choice of a Maslov potential, this holds true for 2-component A -type links as well. The differential is given by (signed) counts of holomorphic disks with punctures at Reeb chords. See [EN19] for a more in-depth discussion of the Legendrian Contact DGA.

The Legendrian contact DGA can be difficult to extract information from, so it is often useful to consider augmentations of the DGA. Augmentations are DGA maps from $\mathcal{A}(\lambda)$ to some ground ring. Here we consider the ground ring of Laurent polynomials in $n - 1$ variables with coefficient ring R , understood as a DGA with trivial differential and concentrated in degree 0. We typically take R to be the ring \mathbb{Z}_2 or \mathbb{Z} . The space of all augmentations of $\mathcal{A}(\lambda)$, denoted by $\text{Aug}(\lambda)$, is also an invariant of λ . In the case where λ is the rainbow closure of a positive braid, $\text{Aug}(\lambda)$ has the structure of an affine algebraic variety and is known as the augmentation variety.

Remark. The DGA is more properly defined with the addition of degree 0 generators t_i represented by marked points on the Legendrian λ . The convention we adopt in this manuscript is to introduce a single marked point for every component. In the case where λ is a knot, Levenson showed that any augmentation of $\mathcal{A}(\lambda)$ sends t to -1 [Lev16], with an appropriate choice of spin structure. When λ is a link, an augmentation sends the product $t_1 t_2$ to -1 . We will always further specialize t_1 to -1 , and thus t_2 gets sent to 1 so that we avoid the appearance of any base points in our computations below. □

In general, an exact Lagrangian filling L of a Legendrian λ induces an augmentation ϵ_L of $\mathcal{A}(\lambda)$ [EHK16]. When the grading of $\mathcal{A}(\lambda)$ is concentrated in nonnegative degrees, as is the case for torus links, then $\text{Aug}(\lambda) \cong \text{Spec } H_0(\mathcal{A}(\lambda))$. Since Spec is contravariant, ϵ_L induces a map $\text{Spec}(R[s_1^{\pm 1}, \dots, s_{n-1}^{\pm 1}]) \rightarrow \text{Spec } H_0(\mathcal{A}(\lambda))$, where we have identified the ground ring of Laurent polynomials with the group ring $R[\mathbb{Z}^{n-1}] \cong R[s_1^{\pm 1}, \dots, s_{n-1}^{\pm 1}]$ for some variables s_1, \dots, s_{n-1} . We interpret this map as the inclusion of a toric chart $\text{Spec}(R[s_1^{\pm 1}, \dots, s_{n-1}^{\pm 1}]) \cong (R^*)^{n-1}$ in the augmentation variety. The image of degree-zero generators under an augmentation give local coordinate

²Note that a precise classification of fillings currently only exists for the Legendrian unknot. In general, it is not known whether every filling is constructible, i.e. can be given as a series of elementary cobordism.

functions on the corresponding toric chart. Subsection 3.2 contains a combinatorial definition of these local toric coordinates for A -type, as originally given in [Pan17].

For $\lambda(A_{n-1})$, the polynomials defining the augmentation variety have a combinatorial description as a specific entry in a product of matrices. These matrices originally appeared in [Kál06] and were used in [CGGS20] to prove a holomorphic symplectic structure on the augmentation variety. We adopt the convention of [CGGS20] and define the braid matrix $B(z_i) = \begin{pmatrix} 0 & 1 \\ 1 & z_i \end{pmatrix}$. The augmentation variety of the max-tb Legendrian $(2, n)$ torus link is then cut out as the zero set of the polynomial

$$X_n := 1 + \left[\prod_{i=1}^n B(z_i) \right]_{2,2}$$

where the subscript denotes the 2, 2 entry of the product and the variable z_i corresponds to the Reeb chord appearing as the i th crossing in the Ng

The braid matrices also define regular functions $\Delta_{i,j}$ on X_n by

$$\Delta_{i,j} := \left[\prod_{i=1}^{j-2} B(z_i) \right]_{2,2}.$$

Upon inspection, it is readily verified that these functions satisfy the recursion relation

$$(1) \quad \Delta_{i,j} = z_i \Delta_{i+1,j} + \Delta_{i+2,j}$$

Equation (1) is precisely the recurrence relation used to define the Euler continuant polynomials referenced in the introduction [Eul64]. As a result, the $\Delta_{i,j}$ also satisfy Euler's identity for continuants,

$$\Delta_{1,\mu+\nu+2} \Delta_{\mu+1,\mu+\kappa+2} - \Delta_{1,\mu+\kappa+2} \Delta_{\mu+1,\mu+\nu+2} = (-1)^{\nu+1} \Delta_{1,\mu+1} \Delta_{\mu+\kappa+2,\mu+\nu+2}$$

for $\mu \geq 1, \kappa \geq 0, \nu \geq \kappa + 1$ [Ust06].

Example. Consider the Legendrian trefoil, $\lambda(A_2)$. The augmentation variety $\text{Aug}(\lambda(A_2))$ is the zero set of the polynomial $X_3 = 1 + z_1 + z_3 + z_1 z_2 z_3$. The regular functions $\Delta_{i,j}$ are of the form $\Delta_{i,i+2} = z_i$ or $\Delta_{i,i+3} = 1 + z_i z_{i+1}$, for $1 \leq i \leq 3$. There are $C_3 = 5$ triangulations of the pentagon, which yield five pairs of $\Delta_{i,j}$ corresponding to diagonals of these triangulations.

2.3. The Kalman loop and related combinatorics. In [Kál05], Kalman defined a geometric operation on Legendrian torus links that induces an action on their exact Lagrangian fillings. This operation consists of a Legendrian isotopy that is visualized by dragging a crossing of λ clockwise around the link. The graph of this isotopy is an exact Lagrangian cylinder in the symplectization of (\mathbb{R}^3, ξ_{st}) . Concatenating this cylinder with a filling L of λ yields another filling, generally not Hamiltonian isotopic to L . As computed in [Kál05], this induces an automorphism ϑ on the augmentation variety $\text{Aug}(\lambda(A_{n-1}))$ defined on generators z_i by $\vartheta(z_i) = z_{i-1}$ for $2 \leq i \leq n$ and

$$\vartheta(z_1) = (-1)^n \alpha := (-1)^n \left[\prod_{i=2}^n B(z_i) \right]_{2,2}.$$

In the $\Delta_{i,j}$ functions, this is expressed as

$$\vartheta(\Delta_{1,j}) = (-1)^n \left[B(\alpha) \prod_{i=1}^{j-3} B(z_i) \right]_{2,2}.$$

In the next section, we will show that in $\text{Aug}(\lambda)$, the global functions $\Delta_{i,j}$ transform as $\vartheta(\Delta_{i,j}) = \Delta_{i-1,j-1}$ for indices taken modulo $n+2$. As suggested by our weave fillings, we can also consider the \mathbb{Z}_{n+2} action of counterclockwise rotation on the set of diagonals $\{D_{i,j}\}_{\mathcal{T}}$ of a triangulation \mathcal{T} of the $(n+2)$ -gon. Restricting to the toric chart induced by an augmentation σ , there is a corresponding triangulation \mathcal{T}_σ for which it can be shown that the set map $D_{i-1,j-1} \mapsto \Delta_{i,j}$ between diagonals $\{D_{i-1,j-1}\}_{\mathcal{T}_\sigma}$ of the triangulation \mathcal{T}_σ and regular functions $\{\Delta_{i,j}\}$ is a \mathbb{Z}_{n+2} -equivariant map. The combinatorics of triangulations will therefore appear as crucial ingredients in the proofs of Theorems 1.2 and 1.3. In the remainder of this section we describe some of these relevant combinatorial characteristics as well as the connection between pinching sequences and triangulations.

The number of orbits of the set of triangulations of the $(n+2)$ -gon under the action of counterclockwise rotation is given by the formula

$$\frac{C_n}{n+2} + \frac{C_{(n)/2}}{2} + \frac{2C_{n/3}}{3}$$

where, as previously, the terms with $C_{n/2}$ and $C_{n/3}$ only appear if the indices are integers. These terms correspond, respectively, to triangulations with no rotational symmetry, rotational symmetry by π , and rotational symmetry by $\frac{2\pi}{3}$. No other rotational symmetry of a triangulation is possible. The orbit sizes are $n+2$, $\frac{n+2}{2}$ and $\frac{n+2}{3}$, where again the corresponding orbit size only occurs if the relevant fraction is an integer.

In anticipation of the proof of Theorem 1.1, we describe the clip sequence bijection between triangulations of the $(n+2)$ -gon and 312-avoiding permutations in S_n given in [Reg13]. For a 312-avoiding permutation σ , we will denote the corresponding triangulation by \mathcal{T}_σ and a diagonal between vertex i and vertex j of \mathcal{T}_σ by $D_{i,j}$. Adopting the terminology of [Reg13], we refer to a triangle in \mathcal{T}_σ with sides $D_{i,i+2}, D_{i,i+1}, D_{i+1,i+2}$, two of which lie on the $(n+2)$ -gon, as an ear of the triangulation. Note that any triangulation must have at least two ears and that the middle vertex of an ear necessarily has no diagonal incident to it.

Given a triangulation of the $(n+2)$ -gon, the clip sequence bijection is defined as follows. First, label the vertices in clockwise order from 1 to $n+2$. Remove the middle vertex of the ear with the smallest label, record the label and delete all edges of the $(n+2)$ -gon incident to the vertex. Repeat this process with the ear whose middle vertex is now the smallest of the remaining vertices in the resulting triangulation of the $n+1$ -gon. Continue this process until no triangles remain. The main result of [Reg13] is that this map is indeed a bijection between the set of 312-avoiding permutations in S_n and triangulations of the $(n+2)$ -gon. To determine the indices of the functions $\Delta_{i,j}$, we add 1 (modulo $n+2$) to each of the vertex indices, where we represent the equivalence class of 0 as $n+2$. See Figure 5 for a computation of the 312-avoiding permutation corresponding to the triangulation dual to the 2-graph example given above.

The combinatorics of triangulations of the $(n+2)$ -gon have previously appeared in constructions of A -type fillings. As explained in [TZ18, CZ21], Legendrian mutation, an operation for generating new fillings, corresponds to exchanging diagonals of a quadrilateral in the original triangulation to form a new triangulation. Such an exchange of diagonals is depicted in Figure 10, and we refer to it as an edge flip or mutation. See Subsection 3.3 for more on the cluster-algebraic interpretation of this operation. The flip graph or associahedron is then defined to have vertices given by triangulations and an edge between two vertices if the triangulations are related by a single edge flip. The diameter of the flip graph was first investigated via geometric methods by Thurston Sleator and Tarjan in [STT88] and later combinatorially by Pournin in [Pou14]. In general the combinatorics of the flip graph are an area of active interest and there is no known algorithm for determining geodesics. In Subsections 5.2 and 5.3, we present a description of the Kalman loop as a sequence

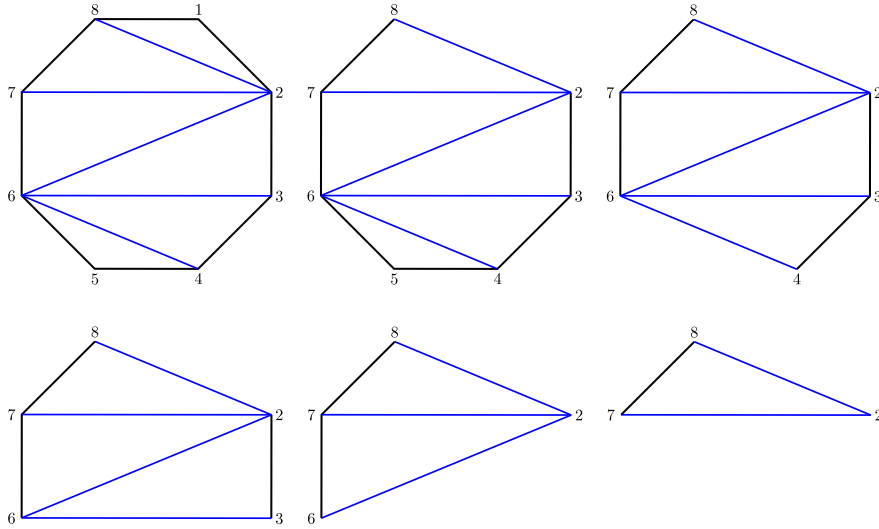


FIGURE 5. An example computation of the clip sequence bijection. Starting with our initial triangulation, we remove and record the smallest numbered vertex with no incident diagonals. From the sequence pictured, we get the 312-avoiding permutation $\sigma = 154362$, where we use one-line notation. The diagonal $D_{2,8}$ yields the function $\Delta_{1,3}$ after adding 1 to both indices and reducing mod 8.

of edge flips in the flip graph and describe the result of a single edge flip on a 312-avoiding permutation, thus providing a characterization of the Kalman loop action as a geodesic path in the flip graph.

3. ALGEBRAIC PROOF OF THEOREM 1.2

In this section we prove Theorem 1.2 by examining the Kalman loop action on the augmentation variety $\text{Aug}(\lambda(A_{n-1}))$ of the Legendrian link $\lambda(A_{n-1})$. As discussed in the previous section, an embedded exact Lagrangian filling yields the inclusion of an algebraic torus into the augmentation variety $\text{Aug}(\lambda(A_{n-1}))$. From [Pan17], we have an explicit computation of a set of coordinate functions s_1, \dots, s_{n-1} on these toric charts coming from pinching sequence fillings; namely, this set of coordinates is in bijection with the relative cycles associated to the unstable manifolds of the saddle critical points for such Lagrangian fillings. Naively, we might hope to distinguish the Hamiltonian isotopy classes of the Lagrangian fillings under the Kalman loop action by studying the associated toric charts and their s_i coordinate functions. In practice these *local* coordinate functions are somewhat difficult to compare under this particular action. Instead, we consider the action of the Kalman loop on the set of *global* regular functions $\{\Delta_{i,j}, \Delta_{i,j} \in R[\text{Aug}(\lambda(A_{n-1}))]\}$, defined in the section above. In fact, $\Delta_{i,j} \in R[z_1, \dots, z_n]$ are globally defined polynomials, which restrict to global regular functions on the augmentation variety $\text{Aug}(\lambda(A_{n-1})) \subseteq R^n$.

When considering the restriction of the $\Delta_{i,j}$ functions to the toric chart induced by the augmentation ϵ_σ , Theorem 3.1 below establishes that the correspondence between diagonals $D_{i-1,j-1}$ of the triangulation \mathcal{T}_σ and the functions $\Delta_{i,j}$ is a \mathbb{Z}_{n+2} -equivariant map. We then show in Subsection 3.2 that the $\Delta_{i,j}$ functions corresponding to diagonals of a triangulation \mathcal{T}_σ restrict to a coordinate basis of the toric chart defined by L_σ . In addition, we give an explicit formula for these coordinate functions as monomials in the s_i local coordinates. It follows that the induced action on the set of augmentations ϵ_σ in the augmentation variety $\text{Aug}(\lambda(A_{n-1}))$ is equivalent to the action of rotation on triangulations of the $(n+2)$ -gon, from which we can conclude the orbital structure as given in Theorem 1.2.(1). See Subsection 3.3 for a cluster-algebraic motivation for the $\Delta_{i,j}$ functions and triangulations of the $(n+2)$ -gon.

3.1. The Kalman loop action on $\{\Delta_{i,j}\}$. Let us start by describing the action of the Kalman loop on the global regular functions $\Delta_{i,j}$ using Euler's identity for continuants. All indices in this section are modulo $n + 2$.

Recall that we denote by $\vartheta \in \text{Aut}(\mathbb{Z}[\text{Aug}(\lambda(A_{n-1}))])$ the automorphism induced by the Kalman loop acting on the augmentation variety $\text{Aug}(\lambda(A_{n-1})) = \{(z_1, \dots, z_n) | X_n = 0\} \subseteq \mathbb{R}^n$, where $X_n \in R[z_1, \dots, z_n]$ is the polynomial defined in Subsection 2.2. The action of the Kalman loop on the set of global regular functions $\{\Delta_{i,j}\}$ is described by the following theorem.

Theorem 3.1. *The set of global regular functions $\Delta_{i,j}$ in $\mathbb{Z}[\text{Aug}(\lambda(A_{n-1}))]$ satisfy the equation*

$$\vartheta(\Delta_{1,k+1}) + (-1)^{n-1} \Delta_{k,n+2} = \Delta_{2,k} (\Delta_{1,n+2} + 1),$$

as global polynomials in ambient \mathbb{R}^n .

Note that restricting to the augmentation variety $\text{Aug}(\lambda(A_{n-1})) = \{X_n = 0\}$ causes the right hand side of the equation to vanish. Therefore, the Kalman loop action on the restriction of $\Delta_{i,j}$ to $\text{Aug}(\lambda(A_{n-1}))$ is $\vartheta(\Delta_{i,j}) = \Delta_{i-1,j-1}$. It follows that the correspondence between $\Delta_{i,j}$ restricted to the toric chart induced by ϵ_σ and a diagonal $D_{i-1,j-1}$ of the triangulation \mathcal{T}_σ is a \mathbb{Z}_{n+2} -equivariant map.

Theorem 1.2.(2) follows from the appearance of Euler's identity for continuants in the proof below.

Proof. We first rewrite the left hand side of the desired equation using the continuant recursion relation (1).

$$\begin{aligned} \vartheta(\Delta_{1,k+1}) + (-1)^{n-1} \Delta_{k,n+2} &= \vartheta(z_1 \Delta_{2,k+1} + \Delta_{3,k+1}) + (-1)^{n-1} \Delta_{k,n+2} \\ &= \alpha \Delta_{1,k} + \Delta_{2,k} + (-1)^{n-1} \Delta_{k,n+2} \\ &= \Delta_{2,n+2} \Delta_{1,k} + \Delta_{2,k} + (-1)^{n-1} \Delta_{k,n+2}. \end{aligned}$$

Therefore, our claim above is equivalent to the expression

$$\Delta_{2,n+2} \Delta_{1,k} + \Delta_{2,k} + (-1)^{n-1} \Delta_{k,n+2} = (\Delta_{1,n+2} + 1) \Delta_{2,k}.$$

Subtracting $\Delta_{2,k}$ from both sides and rearranging some terms yields

$$\Delta_{1,n+2} \Delta_{2,k} - \Delta_{1,k} \Delta_{2,n+2} = (-1)^n \Delta_{k,n+2}.$$

This equation is precisely Euler's identity for continuants with $\mu = 1, \kappa = k - 3, \nu = n - 1$, so Theorem 3.1 follows. \square

3.2. The Kalman loop action on the augmentation variety. We now prove that the $\Delta_{i,j}$ functions, corresponding to the diagonals of the triangulation \mathcal{T}_σ corresponding to the 312-avoiding permutation σ , define a coordinate basis on the toric chart induced by the filling L_σ . To do so, we first show that the $\Delta_{i,j}$ functions can be written as monomials in the local s_i coordinate functions defined by the augmentation ϵ_σ . We then define a bijection between the $\Delta_{i,j}$ corresponding to the triangulation \mathcal{T}_σ and the s_i variables on the toric chart induced by L_σ . Throughout the remainder of this section, let σ denote a 312-avoiding permutation corresponding to a pinching sequence filling and $D_{i,j}$ be a diagonal of the triangulation \mathcal{T}_σ . The goal of this subsection will be to prove the following proposition.

Proposition 3.1. *For any diagonal $D_{i-1,j-1}$ in the triangulation \mathcal{T}_σ , the image of the regular function $\Delta_{i,j}$ in the toric chart induced by the augmentation ϵ_σ is $\epsilon_\sigma(\Delta_{i,j}) = s_i \dots s_{j-2}$.*

Moreover, the set of all $\Delta_{i,j}$ corresponding to the diagonals of the triangulation \mathcal{T}_σ form a basis for the toric chart induced by the augmentation ϵ_σ .

In preparation for the proof of Proposition 3.1, we define the augmentation $\epsilon_\sigma : \mathcal{A}(\lambda(A_{n-1})) \rightarrow \mathbb{Z}_2[s_1^{\pm 1}, \dots, s_{n-1}^{\pm 1}]$. We adopt the notation of [Pan17] and recall the combinatorial formula for the DGA map Φ_i induced by opening the crossing labeled $z_{\sigma(i)}$ of $\lambda(A_{n-1})$. Define the sets

$$\begin{aligned} T_\sigma^i &= \{j \in \{1, \dots, n\} \mid \sigma^{-1}(j) > \sigma^{-1}(i) \text{ and if } i < k < j \text{ or } j < k < i, \text{ then } \sigma^{-1}(k) < \sigma^{-1}(j)\} \\ S_\sigma^i &= \{j \in \{1, \dots, n\} \mid i \in T_\sigma^j\} \\ &= \{j \in \{1, \dots, n\} \mid \sigma^{-1}(j) < \sigma^{-1}(i) \text{ and if } i < k < j \text{ or } j < k < i, \text{ then } \sigma^{-1}(k) < \sigma^{-1}(j)\}. \end{aligned}$$

For $j \in T_\sigma^{\sigma(i)}$ and $1 \leq i \leq n$, the DGA map is given by

$$\Phi_i(z_j) = z_j + s_{\sigma(i)-1} \prod_{\substack{j < k < \sigma(i) \text{ or} \\ \sigma(i) < k < j}} s_k^{-2}$$

and for $j = \sigma(i)$, $\Phi_i(z_j) = s_j$. Otherwise, we take Φ_i to be the identity. The final DGA map Φ_{n+1} is defined as $\Phi_{n+1}(s_n) = s_1^{-1} \dots s_{n-1}^{-1}$ and the identity otherwise.

For a degree-zero generator z_i of $\text{Aug}(\lambda(A_{n-1}))$, the augmentation ϵ_σ is then defined by

$$\epsilon_\sigma(z_i) = \Phi_{n+1} \circ \dots \circ \Phi_1(z_i) = s_i + \sum_{j \in S_\sigma^i} \left(s_j^{-1} \prod_{\substack{j < k < i \text{ or} \\ i < k < j}} s_k^{-2} \right).$$

Example. Given the filling indexed by the 312-avoiding permutation $\sigma = 154362$, consider the function $\Delta_{3,7}$ corresponding to the diagonal $D_{2,6}$ belonging to the triangulation \mathcal{T}_σ , as depicted in Figure 5 above. We have $T_\sigma^1 = \{1, 2\}$ and $T_\sigma^5 = \{4, 6\}$ so that Φ_1 is the identity on $\Delta_{3,7}$ and

$$\Phi_2(\Delta_{3,7}) = \Phi_2(z_3 + z_5 + z_3 z_4 z_5) = s_5 + z_3 z_4 s_5.$$

Continuing with the remaining Φ_i maps of ϵ_σ , yields $\epsilon_\sigma(\Delta_{3,7}) = s_3 s_4 s_5$, as desired.

The technical lemma introduced below will be used to prove the first part of Proposition 3.1.

Lemma 3.1. *For all $0 \leq k \leq n$ and all $i \leq l \leq j-2$ such that $\sigma(l)$ appears in the set $\{\sigma(1), \dots, \sigma(k)\}$, there is a unique term of maximal degree $(j-i-1)$ in the polynomial $\Phi_k \circ \dots \circ \Phi_1(\Delta_{i,j})$ divisible by $s_{\sigma(l)}$. Moreover, $\Phi_n \circ \dots \circ \Phi_1(\Delta_{i,j})$ is a monomial in the variables s_i, \dots, s_{j-2} .*

Assuming the lemma, we first prove Proposition 3.1.

Proof of Proposition 3.1. The lemma above implies that there is a single term of degree $j-i-1$ remaining in the polynomial $\Phi_n \circ \dots \circ \Phi_1(\Delta_{i,j})$ and that it is divisible by $s_i \dots s_{j-2}$. It immediately follows that this term is $s_i \dots s_{j-2}$, proving the first part of Proposition 3.1. To prove the second part, we define a bijection φ between the set of triangles in the triangulation \mathcal{T}_σ and the local toric coordinates s_1, \dots, s_{n-1} induced by the augmentation ϵ_σ . Let T be a triangle in \mathcal{T}_σ with sides $D_{i-1, j-1}, D_{j-1, k-1}$ and $D_{i-1, k-1}$. We define the map φ by

$$\varphi(T) := (\Delta_{i,j})^{-1} (\Delta_{j,k})^{-1} \Delta_{i,k}.$$

where we set $\Delta_{i,i+1} = 1$. By the first part of Proposition 3.1, we have

$$(\Delta_{i,j})^{-1} (\Delta_{j,k})^{-1} \Delta_{i,k} = (s_i \dots s_{j-2})^{-1} (s_j \dots s_{k-2})^{-1} s_i \dots s_{k-2} = s_{j-1}.$$

To see that φ is injective, consider two triangles T and T' belonging to the triangulation \mathcal{T}_σ with sides $\{D_{i-1,j-1}, D_{j-1,k-1}, D_{i-1,k-1}\}$ and $\{D_{i'-1,j'-1}, D_{j'-1,k'-1}, D_{i'-1,k'-1}\}$, respectively. Assume that $\varphi(T) = \varphi(T')$. Then $s_{j-1} = s_{j'-1}$, and therefore $j = j'$. Since T and T' share a middle vertex, and belong to the same triangulation, they must be the same triangle. We can conclude immediately that φ is bijective because it is an injective map between two sets of $n - 1$ elements. Thus, the set of $\Delta_{i,j}$ functions corresponding to diagonals \mathcal{T}_σ form a coordinate basis for the toric chart induced by the augmentation ϵ_σ .

□

We now give a proof of the technical lemma above by induction on the index k of the DGA map Φ_k defining the augmentation ϵ_σ . The overall strategy will be to separate $\Phi_{k-1} \dots \Phi_1(\Delta_{i,j})$ into families of monomials and carefully examine cancellation under Φ_k .

Proof of Lemma 3.1. To simplify notation, we may assume that $\sigma(1), \dots, \sigma(k)$ all lie in the set $\{i, \dots, j - 2\}$. Indeed, for $\sigma(l)$ not in $\{i, \dots, j - 2\}$, the map Φ_l is the identity on the polynomial $\Phi_{l-1} \circ \dots \circ \Phi_1(\Delta_{i,j})$. This follows from the observation that if $D_{i-1,j-1}$ is in the triangulation \mathcal{T}_σ , then i appears before $i - 1$ and $j - 2$ appears before $j - 1$ in σ under the clip sequence bijection. Therefore, $\sigma^{-1}(i) < \sigma^{-1}(i - 1)$ and $\sigma^{-1}(j - 2) < \sigma^{-1}(j - 1)$, which implies that no elements of the set T_σ^l appear in terms of $\Phi_{l-1} \circ \dots \circ \Phi_1(\Delta_{i,j})$.

Beginning with the base case $k = 1$, first note that the set T_σ^1 determining Φ_1 has two elements $\sigma(1) \pm 1$ appearing in $\Delta_{i,j}$ unless $\sigma(1) = i$ or $\sigma(1) = j - 2$. Therefore the three possibilities are $T_\sigma^1 = \{\sigma(1) - 1, \sigma(1) + 1\}$, $T_\sigma^1 = \{i + 1\}$, or $T_\sigma^1 = \{j - 3\}$. For T_σ^k with $k > 1$, we denote the elements of T_σ^k by $\sigma(k) +$ and $\sigma(k) -$, should they exist. We also denote by $\sigma(k) ++$ (respectively, $\sigma(k) --$) the term in $\{i, \dots, j - 2\} \setminus \{\sigma(1), \dots, \sigma(k - 1)\}$ with the next largest (respectively, smallest) index should it exist. We define $\sigma(k) +++$ and $\sigma(k) ---$ analogously.

Before applying Φ_1 to $\Delta_{i,j}$, observe that terms in $\Delta_{i,j}$ are of the form:

- (1) $u_1 z_{\sigma(1)-1} z_{\sigma(1)} z_{\sigma(1)+1} v_1$
- (2) $u_1 \hat{z}_{\sigma(1)-1} \hat{z}_{\sigma(1)} z_{\sigma(1)+1} v_1$
- (3) $u_1 z_{\sigma(1)-1} \hat{z}_{\sigma(1)} \hat{z}_{\sigma(1)+1} v_1$
- (4) $u_1 z_{\sigma(1)-1} z_{\sigma(1)} v_2$
- (5) $u_1 \hat{z}_{\sigma(1)-1} \hat{z}_{\sigma(1)} v_2$
- (6) $u_2 z_{\sigma(1)} z_{\sigma(1)+1} v_1$
- (7) $u_2 \hat{z}_{\sigma(1)} \hat{z}_{\sigma(1)+1} v_1$
- (8) $u_2 z_{\sigma(1)} v_2$

where we denote by \hat{z} a variable removed from the monomial, and u_1, u_2, v_1 and v_2 are monomials in $\Delta_{i,\sigma(1)}$, $\Delta_{i,\sigma(1)-1}$, $\Delta_{\sigma(1)+2,j}$, and $\Delta_{\sigma(1)+3,j}$, respectively. Under Φ_1 , the above terms behave as follows:

- (1) $\Phi_1(u_1 z_{\sigma(1)-1} z_{\sigma(1)} z_{\sigma(1)+1} v_1) = u_1 z_{\sigma(1)-1} s_{\sigma(1)} z_{\sigma(1)+1} v_1 + u_1 z_{\sigma(1)+1} v_1 + u_1 z_{\sigma(1)-1} v_1 + u_1 s_{\sigma(1)}^{-1} v_1$
- (2) $\Phi_1(u_1 \hat{z}_{\sigma(1)-1} \hat{z}_{\sigma(1)} z_{\sigma(1)+1} v_1) = u_1 z_{\sigma(1)+1} v_1 + u_1 s_{\sigma(1)}^{-1} v_1$
- (3) $\Phi_1(u_1 z_{\sigma(1)-1} \hat{z}_{\sigma(1)} \hat{z}_{\sigma(1)+1} v_1) = u_1 z_{\sigma(1)-1} v_1 + u_1 s_{\sigma(1)}^{-1} v_1$
- (4) $\Phi_1(u_1 z_{\sigma(1)-1} z_{\sigma(1)} v_2) = u_1 z_{\sigma(1)-1} s_{\sigma(1)} v_2 + u_1 v_2$
- (5) $\Phi_1(u_1 \hat{z}_{\sigma(1)-1} \hat{z}_{\sigma(1)} v_2) = u_1 v_2$
- (6) $\Phi_1(u_2 z_{\sigma(1)} z_{\sigma(1)+1} v_1) = u_2 s_{\sigma(1)} z_{\sigma(1)+1} v_1 + u_2 v_1$
- (7) $\Phi_1(u_2 \hat{z}_{\sigma(1)} \hat{z}_{\sigma(1)+1} v_1) = u_2 v_1$
- (8) $\Phi_1(u_2 z_{\sigma(1)} v_2) = u_2 s_{\sigma(1)} v_2$.

Examining the result, we see that the $u_1 s_{\sigma(1)}^{-1} v_1$ terms coming from monomial families (2) and (3) cancel with each other, and the $u_1 z_{\sigma(1)\pm 1} v_1$ terms from the monomial family (1) cancel with the remaining terms coming from the monomial families (2) and (3). Similarly, the $u_1 v_2$ terms from the monomial families (4) and (5) cancel, as do the $u_2 v_1$ terms from monomial families (6) and (7). We are then left with terms of the following form:

- (1) $u_1 z_{\sigma(1)-1} s_{\sigma(1)} z_{\sigma(1)+1} v_1$
- (2) $u_1 s_{\sigma(1)}^{-1} v_1$
- (3) $u_1 z_{\sigma(1)-1} s_{\sigma(1)} v_2$
- (4) $u_2 s_{\sigma(1)} z_{\sigma(1)+1} v_1$
- (5) $u_2 s_{\sigma(1)} v_2$.

From this computation, we can see that the terms that cancel are precisely the terms we get when we remove $z_{\sigma(1)-1} z_{\sigma(1)}$ from a term originally containing them. The number of terms of this kind is equal to the number of terms in $\left[B(z_i) \dots \hat{B}(z_{\sigma(1)-1}) \hat{B}(z_{\sigma(1)}) \dots B(z_{j-2}) \right]_{2,2}$ or equivalently, the number of terms in $\Delta_{i,j-2}$. Since $\Delta_{i,i+2}$ has one term, $\Delta_{i,i+3}$ has two terms, and the continuant recursion relation does not cause any cancellation, we can conclude that $\Delta_{i,j}$ has a Fibonacci number F_{j-i} of terms. Therefore, $\Delta_{i,j-2}$ has $F_{(j-2-i)-2}$ terms and the number of remaining terms in $\Phi_1(\Delta_{i,j})$ is $F_{(j-2-i)-1}$.

If $|T_\sigma^1| = 1$, then without loss of generality, assume $\sigma(1) = i$. We get terms of the form

- (1) $z_i z_{i+1} u_1$
- (2) $\hat{z}_i \hat{z}_{i+1} u_1$
- (3) $z_i u_2$

where u_1 a monomial in $\Delta_{\sigma(1)+2,j}$ and u_2 is a monomial in $\Delta_{\sigma(1)+3,j}$. Under Φ_1 , we have:

- (1) $\Phi_1(z_i z_{i+1} u_1) = s_i z_{i+1} u_1 + u_1$
- (2) $\Phi_1(\hat{z}_i \hat{z}_{i+1} u_1) = u_1$
- (3) $\Phi_1(z_i u_2) = s_i u_2$

Upon inspection, the u_1 terms from monomial families (1) and (2) cancel. Therefore, we have an identical computation of the number of terms, as the terms we get by removing a factor of $z_i z_{i+1}$ are the terms in $\Delta_{i+2,j}$.

For $k > 1$, we will consider the case where $|T_\sigma^k| = 2$. The case where $|T_\sigma^k| = 1$ is analogous.

Assume inductively that terms of the polynomial $\Phi_{k-1} \circ \dots \circ \Phi_1(\Delta_{i,j})$ are of the form:

- (1) $u_1 z_{\sigma(k)-z_{\sigma(1)}} z_{\sigma(k)+1} v_1 w_1$
- (2) $u_1 \hat{z}_{\sigma(k)-\hat{z}_{\sigma(k)}} z_{\sigma(k)+1} v_1 w_2$
- (3) $u_1 z_{\sigma(k)-\hat{z}_{\sigma(k)}} \hat{z}_{\sigma(k)+1} v_1 w_3$
- (4) $u_1 z_{\sigma(k)-z_{\sigma(k)}} v_2 w_4$
- (5) $u_1 \hat{z}_{\sigma(k)-\hat{z}_{\sigma(k)}} v_2 w_5$
- (6) $u_2 z_{\sigma(k)} z_{\sigma(k)+1} v_1 w_6$
- (7) $u_2 \hat{z}_{\sigma(k)} \hat{z}_{\sigma(k)+1} v_1 w_7$
- (8) $u_2 z_{\sigma(k)} v_2 w_8$

where we have:

- u_1 is a monomial in $\left[\prod_{l \in \{z_i, \dots, z_{\sigma(k)-1}\} \setminus \{z_{\sigma(1)}, \dots, z_{\sigma(k-1)}\}} B(z_l) \right]_{2,2}$
- u_2 is a monomial in $\left[\prod_{l \in \{z_i, \dots, z_{\sigma(k)-1}\} \setminus \{z_{\sigma(1)}, \dots, z_{\sigma(k-1)}\}} B(z_l) \right]_{2,2}$

- v_1 is a monomial in $\left[\prod_{l \in \{z_{\sigma(k)++}, \dots, z_{j-2}\} \setminus \{z_{\sigma(1)}, \dots, z_{\sigma(k-1)}\}} B(z_l) \right]_{2,2}$
- v_2 is a monomial in $\left[\prod_{l \in \{z_{\sigma(k)+++}, \dots, z_{j-2}\} \setminus \{z_{\sigma(1)}, \dots, z_{\sigma(k-1)}\}} B(z_l) \right]_{2,2}$
- $w_l = s_{\sigma(1)}^{\pm 1} \dots s_{\sigma(k-1)}^{\pm 1}$

Denote by $M_k(m)$ the number such that $\sigma^{-1}(M_k(m))$ is the largest index in $\{1, \dots, k\}$ for which T_σ^m is contained in the set $\{M_k(m)-, \dots, M_k(m)+\}$. The factor $s_{\sigma(m)}^{-1}$ appears in w_l if the monomial is a term in the polynomial

$$P_{m,k-1}(z) := \left[\prod_{q \in \{i, \dots, j-2\} \setminus \{\sigma(1), \dots, \sigma(k-1), z_{M_{k-1}(m)-}, z_{M_{k-1}(m)+}\}} B(z_q) \right]_{2,2}.$$

Otherwise, $s_{\sigma(m)}$ appears in w_l . In particular, the $s_{\sigma(1)}$ factors appearing in $\Phi_1(\Delta_{i,j})$ satisfy these criteria. Note that there is a unique monomial $\left(\prod_{m \in \{i, \dots, j-2\} \setminus \{\sigma(1), \dots, \sigma(k-1)\}} z_m \right) s_{\sigma(1)} \dots s_{\sigma(k-1)}$ in the family (1) that has maximal degree.

Applying the map Φ_k to the monomials above yields:

- (1) $\Phi_k(u_1 z_{\sigma(k)-z_{\sigma(1)} z_{\sigma(k)+} v_1 w_1) = u_1 z_{\sigma(k)-} s_{\sigma(1)} z_{\sigma(k)+} v_1 w_1 + u_1 z_{\sigma(k)+} v_1 w_1' + u_1 z_{\sigma(k)-} v_1 w_1'' + u_1 s_{\sigma(k)}^{-1} v_1 w_1'''$
- (2) $\Phi_k(u_1 \hat{z}_{\sigma(k)-\hat{z}_{\sigma(k)} z_{\sigma(k)+} v_1 w_2) = u_1 z_{\sigma(k)+} v_1 w_2 + u_1 s_{\sigma(k)}^{-1} v_1 w_2'$
- (3) $\Phi_k(u_1 z_{\sigma(k)-\hat{z}_{\sigma(k)} \hat{z}_{\sigma(k)+} v_1 w_3) = u_1 z_{\sigma(k)-} v_1 w_3 + u_1 s_{\sigma(k)}^{-1} v_1 w_3'$
- (4) $\Phi_k(u_1 z_{\sigma(k)-z_{\sigma(k)} v_2 w_4) = u_1 z_{\sigma(k)-} s_{\sigma(k)} v_2 w_4 + u_1 v_2 w_4'$
- (5) $\Phi_k(u_1 \hat{z}_{\sigma(k)-\hat{z}_{\sigma(k)} v_2 w_5) = u_1 v_2 w_5$
- (6) $\Phi_k(u_2 z_{\sigma(k) z_{\sigma(k)+} v_1 w_6) = u_2 s_{\sigma(k)} z_{\sigma(k)+} v_1 w_6 + u_2 v_1 w_6'$
- (7) $\Phi_k(u_2 \hat{z}_{\sigma(k)} \hat{z}_{\sigma(k)+} v_1 w_7) = u_2 v_1 w_7$
- (8) $\Phi_k(u_2 z_{\sigma(k)} v_2 w_8) = u_2 s_{\sigma(k)} v_2 w_8$

where the w_l' terms denote the result of multiplying w_l by any $s_{\sigma(m)}^{-2}$ terms coming from $\Phi_k(z_{\sigma(k)+})$ or $\Phi_k(z_{\sigma(k)-})$.

In order to conclude that these terms cancel as the terms in the $k=1$ case, we need to verify that our description of the w_l terms implies $w_1''' = w_2' = w_3'$, $w_1' = w_2$, $w_1'' = w_3$, $w_4' = w_5$, and $w_6' = w_7$. We handle the case of $w_1' = w_2$. The remaining cases are analogous.

Consider the words w_1 and w_2 . If $s_{\sigma(m)}$ appears in w_1 but $s_{\sigma(m)}^{-1}$ appears in w_2 , then by the criteria defined above, we must have that $z_{\sigma(k)-} = z_{M_k(m)-}$. As a consequence, $\sigma(k) \geq M_k(m)+$ and therefore there is a factor of $s_{\sigma(m)}^{-2}$ in the second term of $\Phi_k(z_{\sigma(k)-})$ so that $S_{\sigma(m)}^{-1}$ appears in both w_1' and w_2 . Otherwise, if $s_{\sigma(m)}^{\pm}$ appears in both w_1 and w_2 , then it appears in w_1' as well and it follows that $w_1' = w_2$.

Therefore, cancellation yields terms of the form:

- (1) $u_1 z_{\sigma(k)-} s_{\sigma(k)} z_{\sigma(k)+} v_1 w_1$
- (2) $u_1 s_{\sigma(k)}^{-1} v_1 w_1'''$
- (3) $u_1 z_{\sigma(k)-} s_{\sigma(k)} v_2 w_4$
- (4) $u_2 s_{\sigma(k)} z_{\sigma(k)+} v_1 w_6$
- (5) $u_2 s_{\sigma(k)} v_2 w_8$

To conclude the proof of the lemma, it remains only to verify that $s_{\sigma(m)}^{-1}$ appears in any of the remaining monomials if and only if that monomial is a term in the polynomial $P_{m,k}(z)$.

If any $s_{\sigma(m)-1}$ appears in an uncanceled term from monomial family (1), (3), (4), or (5), then by the inductive hypothesis, we know that the monomial is a term in $P_{m,k-1}(z)$. Moreover, by our description of Φ_k , we know that $M_{k-1}(m) = M_k(m)$ because neither $z_{M_k(m)+}$ nor $z_{M_k(m)-}$ appear in the monomial. Since we only remove the $\sigma(k)$ index, the result is a term in $P_{m,k}(z)$.

If $s_{\sigma(m)}^{-1}$ appears in w_1 , then the monomial is a term in $P_{m,k-1}(z)$. It follows that the resulting monomial in family (2) is a term in $P_{m,k}(z)$, because we remove $\sigma(k)$ from the indexing set and both $z_{\sigma(k)+}$ and $z_{\sigma(k)-}$ are deleted. Finally, if $s_{\sigma(m)}^{-1}$ does not appear in w_1 , but does appear in w_1''' then the monomial is not a term in $P_{m,k-1}(z)$. Therefore, we must have $z_{\sigma(m)+} = z_{\sigma(k)+}$ and $\sigma(k)- \leq \sigma(m)-$ or $z_{\sigma(m)-} = z_{\sigma(k)-}$ and $\sigma(k)+ \leq \sigma(m)+$. By definition, this means that $M_k(m) = \sigma(k)$, so the resulting monomial is a term in $P_{m,k}(z) = P_{k,k}(z)$.

Now if the original monomial is a term in $P_{m,k-1}(z)$, then $s_{\sigma(m)}^{-1}$ appears in w_l by the inductive hypothesis. Since neither $z_{M_{k-1}(m)+}$ nor $z_{M_{k-1}(m)-}$ appear in the monomial, applying Φ_k does not change the power of $s_{\sigma(m)}$.

Otherwise, if applying Φ_k to a monomial results in a term of $P_{m,k}(z)$ but the original monomial is not a term in $P_{m,k-1}(z)$, then we must have that the monomial is in family (2). Indeed, were this not the case, then the only way this could happen would be if either $\sigma(k) = z_{M_{k-1}(m)+}$ and $\sigma(k)- \leq M_{k-1}(m)-$ or $\sigma(k) = z_{M_{k-1}(m)-}$ and $M_{k-1}(m)+ \leq \sigma(k)+$. Therefore, we would have $M_k(m) = \sigma(k)$, which implies that the resulting monomial is not a term in $P_{m,k}(z)$.

If we have a monomial in family (2) that is a term in $P_{m,k}(z)$ only after applying Φ_k , then we must have either $z_{\sigma(k)-} = z_{M_{k-1}(m)-}$ and $z_{\sigma(k)+} \geq z_{M_{k-1}(m)+}$ or $z_{\sigma(k)+} = z_{M_{k-1}(m)+}$ and $z_{\sigma(k)-} \geq z_{M_{k-1}(m)-}$. Therefore, $M_k(m) = \sigma(k)$, and the resulting monomial is a term in $P_{m,k}(z) = P_{k,k}(z)$. Thus, we have shown that $s_{\sigma(m)}^{-1}$ appears in w_l if and only if the monomial is a term in $P_{m,k}(z)$.

Just as in the base case, the net change is that we have $F_{(j-2-i)-(k+1)}$ fewer terms than the $F_{(j-2-i)-(k-1)}$ terms we started with, leaving us with $F_{(j-2-i)-k}$ terms. Moreover, the unique monomial of maximal degree is now $\left(\prod_{m \in \{i, \dots, j-2\} \setminus \{\sigma(1), \dots, \sigma(k-1), \sigma(k)\}} z_m\right) s_{\sigma(1)} \cdots s_{\sigma(k)}$.

□

3.3. Relation to Clusters. The appearance of the $\Delta_{i,j}$ functions and the combinatorics of the $(n+2)$ -gon is explained by a cluster structure on the augmentation variety, the existence of which was recently proven by Gao-Shen-Weng in [GSW20]. In brief, a cluster variety is an algebraic variety containing a set of toric charts (cluster charts) with coordinate functions (cluster variables) that transform according to a specific operation (cluster mutation) under the chart maps. See [FWZ20a, FWZ20b] for more on cluster algebras.

For a Legendrian λ given as the rainbow closure of a positive braid, [GSW20] describes a cluster structure on $\text{Aug}(\lambda)$ by proving a natural isomorphism to double Bott-Samelson cells. In particular, the cluster structure on $\text{Aug}(\lambda(A_{n-1}))$ is a cluster algebra of A -type. A -type cluster algebras were originally defined and studied by Fomin and Zelevinsky in the context of regular functions on the affine cone of the Grassmanian $Gr^\times(2, n+2)$. If we consider the Plücker coordinate $P_{i,j}$ of the (ordinary) Grassmanian $Gr(2, n+2)$, then its image in the affine cone is precisely the function $\Delta_{i,j}$. The combinatorics of the relationship between cluster charts is captured by the flip graph, where a single cluster seed is given by all $\Delta_{i,j}$ corresponding to diagonals $D_{i,j}$ of a triangulation. In the context of this manuscript, [GSW20] implies the existence of cluster coordinates on $\text{Aug}(\lambda(A_{n-1}))$ while Proposition 3.1 gives a precise formula.

Also of interest in the cluster setting is the fact that the Kalman loop induces a cluster automorphism of the augmentation variety $\text{Aug}(\lambda(A_{n-1}))$. Subsection 5.2 explicitly realizes this automorphism as a sequence of mutations. For an A -type cluster algebra, Assem, Schiffler, and

Shramchenko showed that the cluster automorphism group is \mathbb{Z}_{n+2} [ASS12]. Theorem 3.1 implies that the order of the Kalman loop action on $\text{Aug}(\lambda(A_{n-1}))$ is precisely $n + 2$, so we immediately deduce the following corollary.

Corollary 3.1. *The induced action of the Kalman loop on $\text{Aug}(\lambda(A_{n-1}))$ is a generator of the A -type cluster modular group.*

4. EQUIVALENCE OF D_4^- AND PINCHING COBORDISMS

In this section we prove that a pinching sequence filling L_σ is Hamiltonian isotopic to the weave filling $L_{\mathcal{T}_\sigma}$ for a given 312-avoiding permutation σ . We first show that the pinching cobordism and D_4^- cobordism are Hamiltonian isotopic fixing the boundary.

Proposition 4.1. *The two exact Lagrangian cobordisms we refer to as a pinching cobordism and D_4^- cobordism are Hamiltonian isotopic relative to their boundaries.*

We prove this by giving a local model for the D_4^- cobordism as a sequence of diagrams in both the front and Lagrangian projections and then describing an exact Lagrangian isotopy between the two cobordisms, fixing the boundary. By [FOOO09], this exact Lagrangian isotopy implies the existence of a Hamiltonian isotopy, also fixing the boundary.

We then use Proposition 4.1 to prove that the pinching sequence filling L_σ is Hamiltonian isotopic to the weave filling $L_{\mathcal{T}_\sigma}$. To give an explicit correspondence between crossings resolved via pinching move or D_4^- cobordism, we make use of the vertical weave construction introduced in Subsection 2.1. Theorem 1.1 follows, as the construction of both sets of fillings therefore consists of applying Hamiltonian isotopic elementary cobordisms to remove Reeb chords in the same order.

After proving Proposition 4.1 and Theorem 1.1, we conclude the section with a proof of the orbital structure as a corollary of Theorem 1.1.

Proof of Proposition 4.1. We give two local models of a D_4^- cobordism, depicted in Figures 6 and 7 as slicings in the front (top) and Lagrangian (bottom) projections. The first local model depicts the removal a Reeb chord trapped between a pair of crossings and a 0-resolution of the rightmost crossing. The second local model depicts the removal of a Reeb chord originally appearing to the left of the leftmost crossing and a 0-resolution of this crossing. This is accomplished by first applying a Legendrian isotopy to create a pair of crossings with this Reeb chord trapped between them and proceeding as in the first local model. The main difficulty in our comparison of these local models to the pinching cobordism is to unambiguously relate the Reeb chord removed in the D_4^- cobordism to the Reeb chord removed in the pinching cobordism. This means that we must carefully manipulate the slope of the Legendrian in the front projection to ensure that no new Reeb chords are introduced throughout the process. The local models allow us to verify by inspection that no new Reeb chords appear at any point in this cobordism, as the slopes of the front projection are specified so that no new intersections appear in the Lagrangian projection.

Having given a local model for the slicing of the D_4^- cobordism, we now describe an exact Lagrangian isotopy between this local model and the pinching move cobordism. Starting in the front projection of $\lambda(A_{n-1})$, a slicing of the pinching move cobordism, as defined in Subsection 2.1, consists of applying the Ng resolution, resolving a crossing, and then undoing the Ng resolution. If we restrict our attention to a neighborhood of the contractible Reeb chord we wish to remove, then the exact Lagrangian isotopy between the two cobordisms is visible when examining the Lagrangian

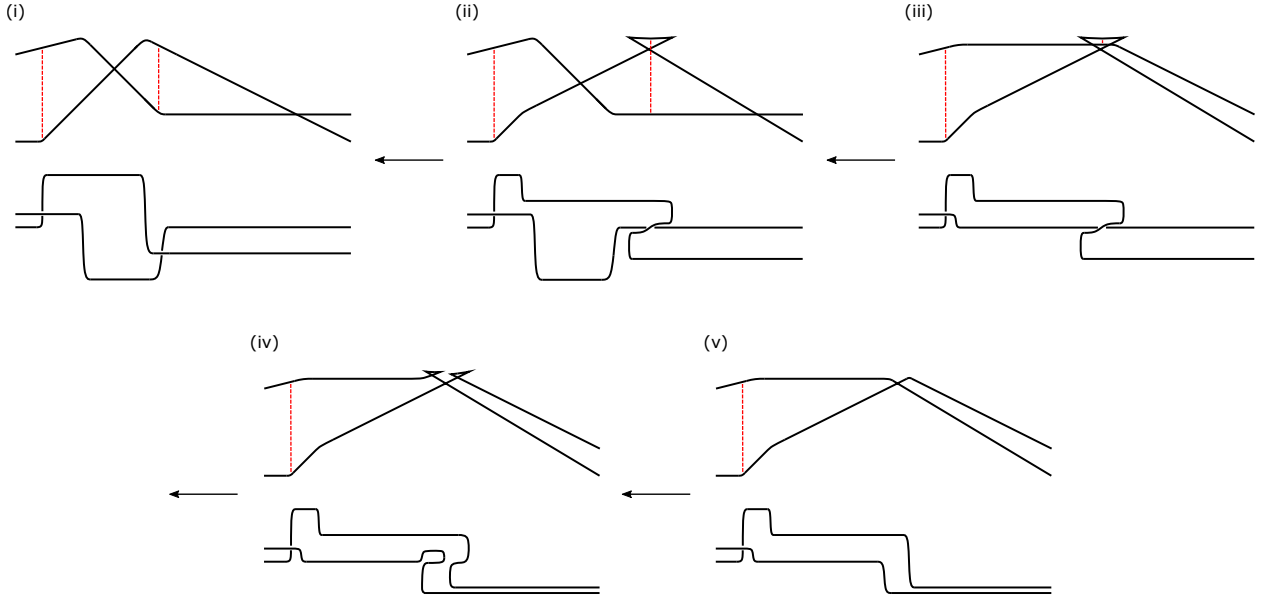


FIGURE 6. Local model of a D_4^- cobordism applied to a pair of crossings in the front (top) and Lagrangian (bottom) projections. Reeb chords are depicted by red dashed lines. The direction of the arrows indicate a cobordism from the concave end to the convex end.

projection of the local models depicted in Figures 6 and 7 (bottom). consists of incrementally rotating the crossing before pinching. Indeed, after applying the Ng resolution, the only difference between these local models and the pinching cobordism in the Ng resolution is the rotating of the strand before resolving. Therefore, the movie of movies realizing the exact Lagrangian isotopy from the D_4^- cobordism to the pinching move cobordism consists of incrementally applying the Legendrian isotopy of the Ng resolution, rotating the crossing before pinching, and then undoing the Ng resolution.

□

To complete the proof of Theorem 1.1 we argue that the clip sequence bijection defined in Subsection 2.3 gives a one-to-one correspondence between fillings that resolves crossings in the same order.

Proof of Theorem 1.1. Let σ be a 312-avoiding permutation indexing a pinching sequence filling L_σ of $\lambda(A_{n-1})$ and consider the vertical weave corresponding to the triangulation \mathcal{T}_σ . By construction, a 0-resolution at the crossing i in $\lambda(A_{n-1})$ corresponds to a trivalent vertex where the incident rightmost edge is labeled by i . By Proposition 4.1, these denote Hamiltonian isotopic exact Lagrangian cobordisms applied to corresponding Reeb chords. Thus, the filling L_σ is Hamiltonian isotopic to the weave filling dual to the triangulation \mathcal{T}_σ .

□

We conclude with a proof of the orbital structure described in Theorem 1.2.(1) as a corollary of Theorem 1.1. Namely, the orbital structure of the Kalman loop action on pinching sequence fillings of $\lambda(A_{n-1})$ can be obtained from the Hamiltonian isotopy between the pinching sequence filling L_σ and weave filling $L_{\mathcal{T}_\sigma}$.

Proof of Theorem 1.2.(1). Let L_σ be a filling of $\lambda(A_{n-1})$ and consider the Hamiltonian isotopic weave filling $L_{\mathcal{T}_\sigma}$ with corresponding 2-graph Γ dual to the triangulation \mathcal{T}_σ . The Kalman loop action on weave fillings is geometrically described as a cylinder rotating the entire 2-graph Γ by $\frac{2\pi}{n+2}$

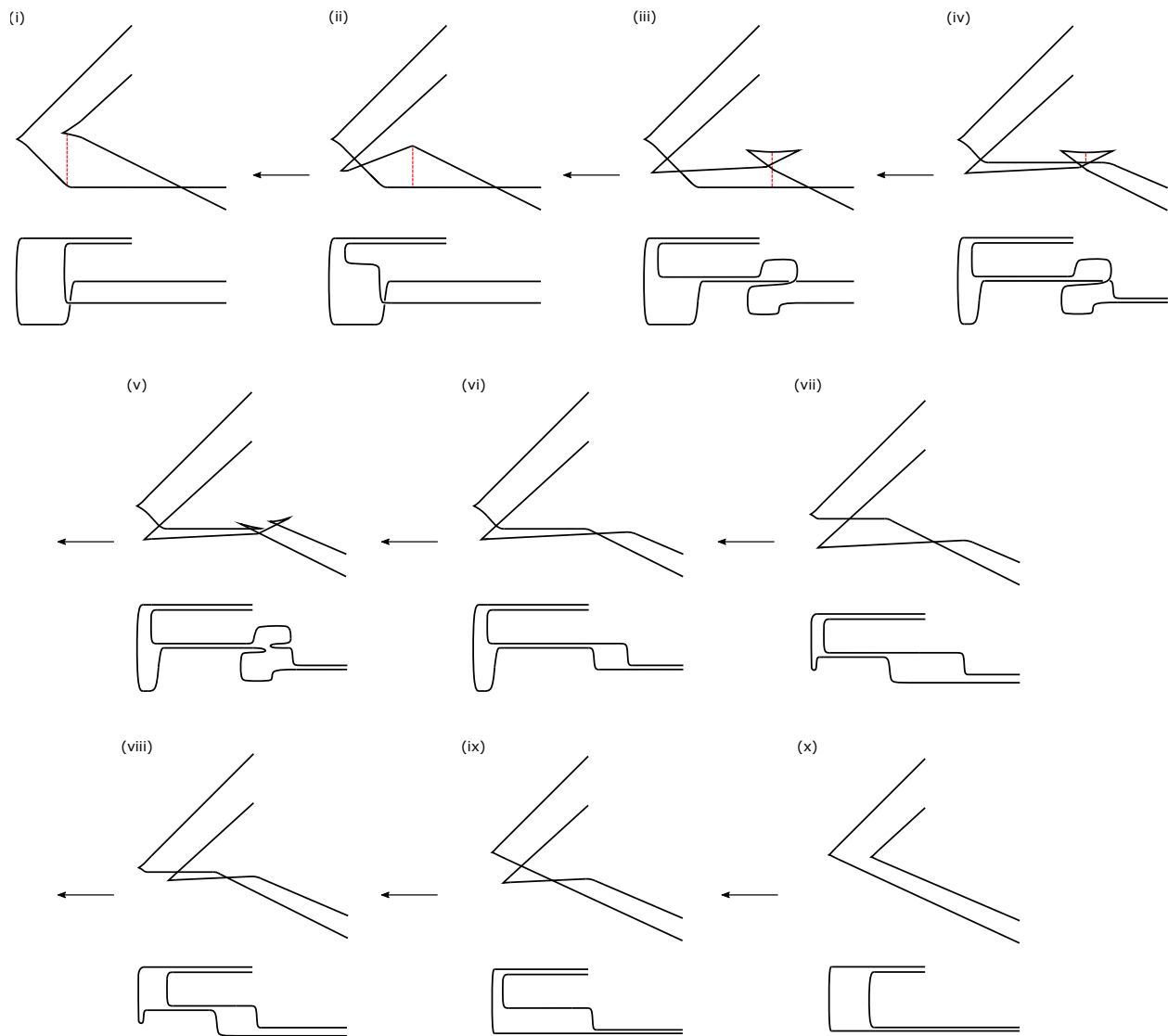


FIGURE 7. Local model of the leftmost crossing in the front (top) and Lagrangian (bottom) projections with a single Reeb chord depicted by a red dashed line. We first apply a Reidemeister II move in order to artificially introduce an additional crossing so that there is a single Reeb chord trapped between the new crossing and the original crossing. The D_4^- cobordism is performed in (iii)-(vi) and the remaining part of the cobordism undoes the Reidemeister II move without creating any new Reeb chords.

radians counterclockwise. This can be readily observed from the fact that crossings of $\lambda(A_{n-1})$ are represented by edges of the dual graph intersecting the boundary of the $(n+2)$ -gon. Therefore, the correspondence between triangulations \mathcal{T}_σ and weave fillings $L_{\mathcal{T}_\sigma}$ implies that the orbital structures of triangulations under the action of rotation and weave fillings under the action of the Kalman loop coincide. \square

Note here the appearance of $\lambda(A_{n-1})$ as the (-1) -framed closure of the braid σ^{n+2} in the description of the weave filling. This geometrically describes why the Kalman loop action on the rainbow closure of σ^n has order $n+2$ as an action on the $n+2$ crossings of the (-1) -framed closure.

5. COMBINATORIAL CHARACTERIZATIONS

In this section, we describe the combinatorial properties of the Kalman loop action on a pinching sequence filling L_σ of $\lambda(A_{n-1})$ purely in terms of the corresponding 312-avoiding permutation σ . We first present an explicit algorithm for determining the orbit size of L_σ from σ in Subsection 5.1. The end of the subsection includes a table where orbit sizes are computed for the case $n = 4$, corresponding to triangulations of the hexagon. We then give a recipe for constructing a geodesic path in the flip graph that describes a counterclockwise rotation of the triangulation \mathcal{T}_σ . Since the weave filling $L_{\mathcal{T}_\sigma}$ is Hamiltonian isotopic to the pinching sequence filling L_σ by Theorem 1.1, this geodesic path describes the Kalman loop action on L_σ as a sequence of edge flips. Finally, we discuss the behavior of 312-avoiding permutations under a single edge flip in the flip graph. Together, these last two results give a combinatorial characterization of the Kalman loop action on fillings purely in terms of 312-avoiding permutations. As in previous sections, all indices are computed modulo $n + 2$.

5.1. Orbit size. The orbit size algorithm of Theorem 1.3 gives explicit criteria for when a filling of $\lambda(A_{n-1})$ has orbit size $\frac{n+2}{2}$ or $\frac{n+2}{3}$ under the action of the Kalman loop. If it does not satisfy either of these criteria, then it necessarily has orbit size $n + 2$. We start by describing the permutations that arise from an orbit of size $\frac{n+2}{2}$.

Consider some 312-avoiding permutation $\sigma \in S_n$. In order for the filling L_σ to have orbit size $\frac{n+2}{2}$, the triangulation \mathcal{T}_σ must have rotational symmetry through an angle of π . Therefore, \mathcal{T}_σ has a diameter $D_{i, i+\frac{n+2}{2}}$ and the triangulated polygons on either side of this diameter must be mirror images. We consider the diameter as an external edge of two $(\frac{n+2}{2} + 1)$ -gons, one containing both vertices labeled $n + 1$ and $n + 2$, and the other containing at most one of them. We denote the latter triangulation by \mathcal{T}_τ where τ is a 312-avoiding permutation in the letters $i + 1, \dots, i + \frac{n+2}{2} - 1$ obtained from applying the clip sequence bijection to this triangulation.

Given an arbitrary 312-avoiding permutation σ in S_n , there may be letters of σ that appear before τ if such a subword even exists. Therefore, to identify τ as a subword of σ we search for the first 312-avoiding permutation of length $\frac{n}{2}$ that appears in σ . A diameter $D_{i, i+\frac{n+2}{2}}$ forces the condition that any letters appearing before τ will be less than i , so that even if i appears directly after τ , there is no ambiguity in identifying τ . If no such τ exists, then the triangulation \mathcal{T}_σ does not have the required rotational symmetry, and therefore σ does not have orbit size $\frac{n+2}{2}$.

We first state a preparatory lemma regarding details of the clip sequence bijection that may give some insight into the structure of the orbit size algorithm below. We consider the most general case where \mathcal{T}_τ is a subtriangulation of \mathcal{T}_σ with vertices $i, \dots, i + k$ for $i + k \leq n + 1$.

Lemma 5.1. *The 312-avoiding permutation τ ends in the letter j if and only if the subtriangulation \mathcal{T}_τ contains the triangle labeled by vertices i, j , and $i+k$. In this case, all letters taking values strictly between i and j appear before any other letters in τ .*

Proof. The first claim follows from the definition of the clip sequence bijection because the diagonal $D_{i, i+k}$ must appear in the final triangle remaining after removing the previous $n - 1$ vertices. Therefore, j is the final letter of τ , if and only if it is also the third vertex of this triangle.

The second claim follows by similar reasoning to the case of the diameter, as the existence of the diagonal $D_{i, j}$ implies that there must be some ear $D_{l, l+2}$ with $i < l < j - 2$. Therefore, $l + 1$ appears before j and we can repeat this argument for the subtriangulation of \mathcal{T}_τ obtained by removing the vertex $l + 1$. \square

We now give explicit criteria for determining whether the filling L_σ has orbit size $\frac{n+2}{2}$ solely in terms of σ .

Lemma 5.2. *The following algorithm detects whether a 312-avoiding permutation σ in S_n yields a filling L_σ of orbit size $\frac{n+2}{2}$ under the action of the Kalman loop.*

- (1) Define σ' to be an empty string and set $\tau' = \tau$. Find the smallest j for which $j \geq \frac{n+2}{2}$ and some $k > j$ appears before j in τ . For the first such k appearing in τ' , append $k - \frac{n+2}{2}$ to σ' , remove k from τ' and repeat until no such letters remain in τ' . Append τ to σ' .
- (2) While τ' ends in the largest (resp. smallest) number remaining in τ' not equal to $\frac{n+2}{2} - 1$ (resp. $\frac{n+2}{2}$), then append the next largest (resp. next smallest) number remaining in $\{1, \dots, n\}$ less than the smallest number (resp. greater than the largest number) of τ' to σ' and delete the final number of τ' .
- (3) If τ' does not end in the largest or smallest remaining number, then add $\frac{n+2}{2}$ to all numbers less than the final number and append to σ' in the order they appear. Delete the corresponding numbers from τ' .
- (4) Now τ' ends in the smallest remaining number, so return to Step (3) and repeat until only one number remains in τ' . The final number of σ' is then uniquely determined by whichever number in $\{1, \dots, n\}$ has not yet been appended.
- (5) σ has orbit size $\frac{n+2}{2}$ if it is equal to σ' .

Example. Consider the 312-avoiding permutation $\sigma = 154362$. We can identify $\tau = 543$ as the first length 3 subword appearing in σ and the diameter of the triangulation \mathcal{T}_σ is therefore $D_{2,6}$. Applying the above algorithm to τ , we see that step (1) yields $\sigma' = 1543$ because 5 precedes 4. Then 3 is the smallest number appearing in τ , so we append 6 to σ' . Finally, we append 2, to get $\sigma = \sigma'$, indicating that the filling labeled by σ has orbit size 4 under the Kalman loop.

Proof. Let $\sigma \in S_n$ be a 312-avoiding permutation with orbit size $\frac{n+2}{2}$. Denote the diameter of \mathcal{T}_σ as $D_{i, i + \frac{n+2}{2}}$ for some $1 \leq i \leq \frac{n+2}{2} - 1$ and the permutation corresponding to the triangulation of the $(\frac{n+2}{2} + 1)$ -gon given by the vertices $i, \dots, i + \frac{n+2}{2}$ by τ . We will show that the algorithm detects when the triangulation \mathcal{T}_σ is obtained from the triangulation \mathcal{T}_τ by gluing \mathcal{T}_τ to a rotation of \mathcal{T}_τ by π along the diagonal $D_{i, i + \frac{n+2}{2}}$. The lemma then follows from the observation that τ is uniquely determined from σ .

Under the clip sequence bijection, we delete the smallest vertex with no incident diagonal at each step and append the label to the permutation. Therefore, any letter k of σ appearing before τ is less than i . Moreover, any diagonal $D_{j,k}$ or $D_{k,j}$ (should it exist) incident to the vertex k has endpoint j in the set $\{n+2, 1, \dots, i\}$. Therefore any triangle with vertices j, k, l with j, k, l given in clockwise order must also have $j, l \in \{n+2, 1, \dots, i\}$. The rotational symmetry of \mathcal{T}_σ implies that the triangle with vertices $j + \frac{n+2}{2}, k + \frac{n+2}{2}, l + \frac{n+2}{2}$ appears in \mathcal{T}_τ . It follows from Lemma 5.1 that in τ the letter $k + \frac{n+2}{2}$ precedes j for some $j \geq \frac{n+2}{2}$ and that all such k appear before τ in σ . Therefore, Step (1) produces all letters of σ that appear before τ .

To determine the letters following τ in σ , we first consider the case where one of the diameter vertices, i or $i + \frac{n+2}{2}$, has no incident diagonals with endpoint taking values in the set of vertices labeled by letters appearing after τ in σ . If this is the case, then the appropriate diameter vertex label immediately follows τ in σ under the clip sequence bijection. We also observe that when i (respectively, $i + \frac{n+2}{2}$) is such a vertex, then there is a triangle in \mathcal{T}_σ with vertices $i, i - 1$, and $i + \frac{n+2}{2}$ (resp. $i, i + \frac{n+2}{2}, i + \frac{n+2}{2} + 1$). Therefore, the rotational symmetry of \mathcal{T}_σ implies that we have a triangle with vertices $i, i + \frac{n+2}{2} - 1$ and $i + \frac{n+2}{2}$ (resp. $i, i + 1$, and $i + \frac{n+2}{2}$) in \mathcal{T}_τ . By Lemma 5.1, the vertex $i + \frac{n+2}{2} - 1$ (resp. $i + 1$) appears as the final letter in τ . The vertex $i - 1$ (resp. $i + \frac{n+2}{2} + 1$) then appears immediately following τ . The same reasoning applies if we replace the diameter $D_{i, i + \frac{n+2}{2}}$ with the diagonal $D_{i-1, i + \frac{n+2}{2}}, D_{i, i + \frac{n+2}{2} + 1}$, or any such longest remaining diagonal arising under the clip sequence bijection in this way, so long as $n + 1$ or $n + 2$ do not appear as endpoints of this diagonal.

If both diameter vertices have diagonals incident to them with endpoints in the remaining vertices, then the letter following τ under the clip sequence bijection labels the smallest vertex greater than $i + \frac{n+2}{2}$ with no incident diagonals. By previous reasoning, we know that the diameter is one side of a triangle with vertices $i, k, i + \frac{n+2}{2}$ in \mathcal{T}_σ . The rotational symmetry of \mathcal{T}_σ implies that the triangle labeled by $i, k - \frac{n+2}{2}, i + \frac{n+2}{2}$ appears in \mathcal{T}_τ . It follows from Lemma 5.1 that k appears as the final letter of τ and any letter j with $j < k$ appearing before k in τ

This process continues until we have eliminated all numbers from τ except for either $n+1$ or $n+2$. This unambiguously determines the final number of our permutation. By construction, we have shown that the above algorithm yields the 312-avoiding permutation σ with \mathcal{T}_σ constructed by gluing a rotated copy of \mathcal{T}_τ to \mathcal{T}_τ .

□

We now consider the case of a 312-avoiding permutation σ with orbit size $\frac{n+2}{3}$. In order to exhibit the appropriate rotational symmetry, the triangulation \mathcal{T}_σ must have a central triangle labeled by vertices $i, i + \frac{n+2}{3}, i + \frac{2(n+2)}{3}$, dividing the triangulation up into three identical triangulations of $(\frac{n+2}{3} + 1)$ -gons. Two of these polygons do not contain the pair of vertices $n+1$ and $n+2$, so a permutation σ with \mathcal{T}_σ having rotational symmetry through an angle of $\frac{2\pi}{3}$ must have two subwords τ_1 and τ_2 of length $\frac{n+2}{3} - 1$ that differ by $\frac{n+2}{3}$ and are immediately followed by $i + \frac{n+2}{3}$. We determine the third subword from τ_1 using the same reasoning as in the $\frac{n+2}{2}$ orbit size case. This yields the following lemma.

Lemma 5.3. *The following algorithm detects whether a 312-avoiding permutation σ in S_n yields a filling L_σ of orbit size $\frac{n+2}{3}$ under the action of the Kalman loop.*

- (1) Determine τ_1 by finding the first subword of length $\frac{n+2}{3} - 1$ in σ with letters $i, \dots, i + \frac{n+2}{3} - 1$ for some i . If no such τ_1 exists, then σ does not have orbit size $\frac{n+2}{3}$.
- (2) For any numbers greater than $\frac{n+2}{3}$ that appear after $\frac{n+2}{3}$ or some other number greater than $\frac{n+2}{3}$, add $\frac{2(n+2)}{3} \pmod{n+2}$ to them and add the result to an empty string along with τ_1 . Add $\frac{n+2}{3}$ to each entry of τ_1 to get τ_2 and append. Append $i + \frac{n+2}{3}$. Delete the corresponding numbers from τ_1 .
- (3) So long as τ_1 ends in the largest (resp. smallest) number remaining in τ_1 not equal to $\frac{n+2}{3} - 1$ (resp. $\frac{n+2}{3}$), then append the next largest (resp. next smallest) number remaining in $\{1, \dots, n\}$ less than the smallest number (resp. greater than the largest number) of τ_1 and delete the final number in τ_1 .
- (4) If τ_1 does not yet end in the largest or smallest remaining number, add $\frac{n+2}{3}$ to all numbers less than the final number and append. Delete the corresponding numbers from τ_1 .
- (5) Now τ_1 ends in the smallest remaining number, so return to the previous step and continue until one number remains in τ_1 . The final number is then uniquely determined by whichever number in $\{1, \dots, n\}$ that has not yet been appended.
- (6) σ has orbit size $\frac{n+2}{3}$ if it is equal to the resulting 312-avoiding permutation

Example. We can identify $\sigma = 2154367$ as a permutation with orbit size $\frac{7+2}{3} = 3$ using the above algorithm. We first identify τ_1 as the first length 2 subword with two consecutive letters. So $\tau_1 = 21 \in S_2$. Then $\tau_2 = 54$ and the string 21543 must appear in σ in order for it to have orbit size 3. We can also determine that no letters appear before τ_1 because 1 and 2 already appear in our word. Since τ_1 ends with the smallest letter of the triangulation \mathcal{T}_{τ_1} , we append 6. The final remaining number is 7, so we see that $\sigma' = \sigma$ and therefore σ has orbit size 3.

We conclude this subsection with a table of orbit sizes of pinching sequence fillings of $\lambda(A_3)$, i.e. the case $n = 4$.

Permutation	Orbit Size
1 2 3 4	6
1 2 4 3	3
1 3 2 4	2
1 3 4 2	6
1 4 3 2	3
2 1 3 4	3
2 1 4 3	6
2 3 1 4	3
2 3 4 1	6
2 4 3 1	2
3 2 1 4	6
3 2 4 1	3
3 4 2 1	3
4 3 2 1	6

5.2. Rotations of Triangulations. In this subsection, we describe a counterclockwise rotation of the $(n + 2)$ -gon through an angle of $\frac{2\pi}{n+2}$ as a geodesic path in the flip graph. We refer to any triangle with edges made up solely of diagonals $D_{i,i+j}$ for $j \geq 2$ as an internal triangle, and we denote the number of internal triangles in a triangulation \mathcal{T}_σ by t_σ .

Given a triangulation \mathcal{T}_σ , the following algorithm describes a sequence of $n - 1 + t_\sigma$ edge flips that produce a rotation of \mathcal{T}_σ by $\frac{2\pi}{n+2}$ radians in the counterclockwise direction. We will say that a diagonal $D_{i,j}$ is (counter)clockwise to another diagonal $D_{i',j'}$ if the vertex j is (counter)clockwise to j' . Similarly, $D_{i,j}$ is (counter)clockwise to $D_{i',j}$ if i is (counter)clockwise to i' .

- (1) For any diagonals $D_{i,j}$ with no incident diagonal counterclockwise to it, perform an edge flip at $D_{i,j}$ to get $D_{i-1,j-1}$. Continue to flip any such diagonals not previously flipped until no such diagonals remain.
- (2) Choose an internal triangle T with a diagonal $D_{i,j}$ not previously flipped and admitting no incident diagonal $D_{i',j}$ counterclockwise to it. Perform an edge flip at $D_{i,j}$ and then flip any diagonals not previously flipped that have no incident counterclockwise diagonals.
- (3) If a diagonal $D_{i',j'}$ of T does have incident counterclockwise diagonals, then perform an edge flip at the counterclockwise-most of these incident diagonals. Flip any diagonals not previously flipped that now admit no incident counterclockwise diagonals.
- (4) Repeat Step (3) until no diagonals counterclockwise to $D_{i',j'}$ remain. Perform an edge flip at $D_{i',j'}$. Once the second and third diagonals of T have been flipped, perform an edge flip at the initial diagonal previously belonging to T .
- (5) Repeat Steps (3) and (4) starting with the remaining diagonals in the triangle corresponding to the counterclockwise diagonal flipped in Step (3). Continue until all possible diagonals have been flipped at.

Theorem 5.1. *The number of edge flips required to realize a counterclockwise rotation of a triangulation \mathcal{T}_σ of the $(n + 2)$ -gon by $\frac{2\pi}{n+2}$ is $n - 1 + t_\sigma$. The above instructions describe an explicit sequence of $n - 1 + t_\sigma$ edge flips realizing such a rotation.*

Proof. We first argue that the number of flips needed to rotate a triangulation is at least $n - 1 + t_\sigma$. Since no diagonal of our original triangulation is a diagonal of our rotated triangulation, a rotation of the triangulation \mathcal{T}_σ requires at least $n - 1$ edge flips, i.e. as many edge flips as diagonals of \mathcal{T}_σ . However, in an internal triangle, it is not possible to apply a single edge flip to any of the three sides (or any other diagonal) so that the result is a side of the rotated triangle, or indeed any diagonal of the rotated triangulation. This is because each of the three sides prevents the side immediately counterclockwise to it from rotating in a counterclockwise direction. If none of the

internal triangles share a side, then the claim follows. Otherwise, we argue that any two triangles sharing an edge still require at least two extra edge flips to rotate. The only possible way we could have fewer is if we could perform an edge flip at the shared side and then rotate the two triangles with a single edge flip of each of the remaining sides. However, if we apply an edge flip at the shared side, then the remaining sides of the two triangles prevent the opposite pair from achieving the desired rotation. Therefore, we must have at least $n - 1 + t_\sigma$ edge flips for a rotation of $\frac{2\pi}{n+2}$.

The algorithm given above describes a path in the flip graph of length $n - 1 + t_\sigma$ since we have two edge flips for a single diagonal in each internal triangle and one for every other diagonal. It remains to show that the result is a rotation of the initial triangulation \mathcal{T}_σ . In Step (1), an edge flip at a diagonal $D_{i,j}$ results in the diagonal $D_{i-1,j-1}$ precisely because there are no diagonals counterclockwise to it and therefore $D_{i,j}$ is a diagonal of the quadrilateral with sides $D_{i,j-1}, D_{j-1,j}, D_{i-1,j}, D_{i-1,i}$. It follows that each edge flip in Step (1) results in a diagonal of the rotated triangulation. If the triangulation \mathcal{T}_σ has no internal triangles, then applying Step (1) to each of the $n - 1$ diagonals results in the desired rotation.

Suppose that \mathcal{T}_σ has at least one internal triangle. In Step (2), an edge flip at the diagonal $D_{i,j}$ in an internal triangle $\{D_{i,j}, D_{j,k}, D_{i,k}\}$ with no diagonal counterclockwise to it, results in the diagonal $D_{j-1,k}$. Once the remaining diagonals of the triangle have no incident counterclockwise diagonals, Step (4) applies an edge flip to them so that $D_{i,k}$ becomes $D_{i-1,j-1}$ and $D_{j,k}$ becomes $D_{j-1,k-1}$. Step (4) then flips $D_{j-1,k}$ to $D_{i-1,k-1}$. Crucially, the order of edge flips ensures that during Steps (2)-(4), we strictly decrease the number of counterclockwise incident diagonals to $D_{j,k}$ and $D_{i,k}$ at each step. After rotating our initial triangle, we can continue this process with the next internal triangle.

It remains to show that in Step (2), a diagonal $D_{i,j}$ of an internal triangle with no incident counterclockwise diagonals $D_{i',j}$ always exists. If $D_{i,j}$ has an incident counterclockwise diagonal not belonging to an internal triangle, then Step (1) will apply an edge flip at such a diagonal so that it is no longer counterclockwise to $D_{i,j}$. If $D_{i,j}$ has an incident counterclockwise diagonal that belongs to an internal triangle, then there is some counterclockwise-most diagonal $D_{i,j'}$ also belonging to an internal triangle. Note that an edge flip at $D_{i,j'}$ removes one of the diagonals counterclockwise to $D_{i,j}$, so we can repeat this argument until we have performed an edge flip at all such diagonals. \square

Example. If the triangulation \mathcal{T}_σ only contains diagonals of the form $D_{i,j_1}, \dots, D_{i,j_{n-1}}$, then the instructions reduce to simply performing edge flips in reverse order of indexing, starting with $D_{i,j_{n-1}}$ and ending with D_{i,j_1} . See Figure 5.2 for a more involved example with three internal triangles.

Remark. For triangulations that allow for a choice of ordering edge flips, it follows from a theorem of Pournin's [Pou14, Theorem 2] that naively proceeding with any of the equivalent options will still yield a geodesic. We can reinterpret this in the cluster algebraic setting as the fact that distant mutations commute. In this context, any geodesic path gives the mutations describing the cluster automorphism induced by the Kalman loop. \square

5.3. Edge flips at a single diagonal. In this subsection, we describe an edge flip at a diagonal $D_{j,l}$ of the triangulation \mathcal{T}_σ in terms of the 312-avoiding permutation σ .

Let $\sigma \in S_n$ be a 312-avoiding permutation with corresponding triangulation given by the clip sequence bijection. Consider a quadrilateral with sides $D_{i,j}, D_{j,k}, D_{k,l}$ and $D_{i,l}$ appearing in the triangulation \mathcal{T}_σ . Figure 9 depicts this quadrilateral with two possible diagonals, $D_{i,k}$ and $D_{j,l}$, separating it into two triangles. An edge flip at one of these diagonals yields the other.

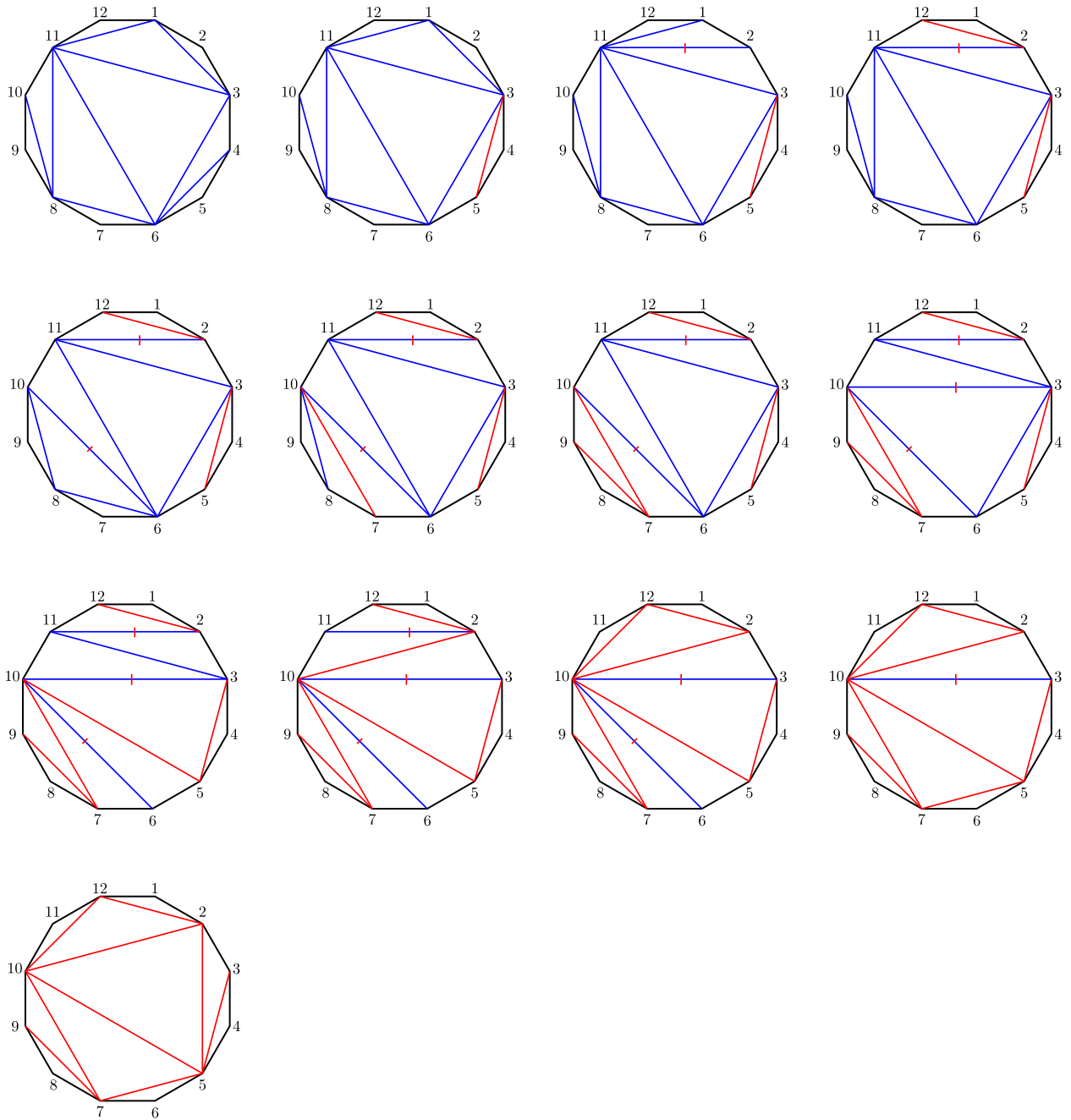


FIGURE 8. Counterclockwise rotation of a triangulation of the 12-gon by $10-1+3=12$ edge flips. The red diagonals are diagonals of the rotated triangulation, while the blue diagonals with a red mark are diagonals that are the result of a previous edge flip but are not diagonals of the rotated triangulation.

As in the orbit size algorithm, we can determine the structure of σ based on the existence of the edges of the quadrilateral. Specifically, σ admits subwords τ_1, τ_2 , and τ_3 , where the subword τ_1 contains the letters $i+1, \dots, j-1$, the subword τ_2 contains letters $j+1, k-1$, and the subword τ_3 contains letters $k+1, \dots, l-1$. From this construction, we can deduce the effect on σ of a single edge flip at $D_{i,j}$.

Theorem 5.2. *Given a triangulation \mathcal{T}_σ containing a quadrilateral with diagonal $D_{i,k}$, the 312-avoiding permutation σ is of the form $\dots\tau_1\tau_2j\tau_3k\dots$. An edge flip at the diagonal $D_{j,l}$ yields a permutation of the form $\dots\tau_1\tau_2\tau_3kj\dots$*

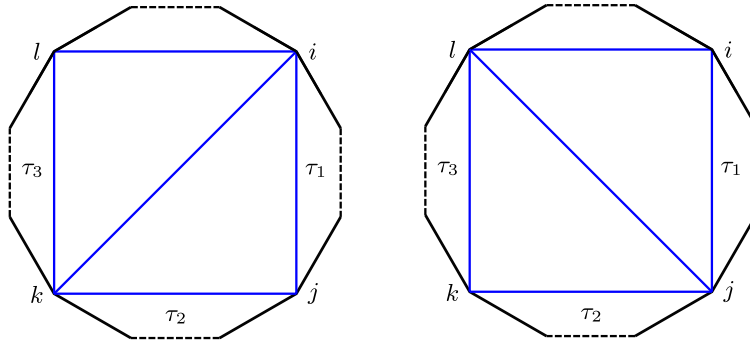


FIGURE 9. Schematic of an edge flip depicting the triangulation \mathcal{T}_σ (left) and the result of applying an edge flip to \mathcal{T}_σ at $D_{i,k}$ (right). The dotted lines represent arbitrarily many edges of the $(n+2)$ -gon and the indices are chosen so that either $1 \leq i < j < k < l \leq n+1$ or $j < k < l = n+1, i = n+2$. The labels τ_1, τ_2 , and τ_3 represent subwords of σ corresponding to different section of \mathcal{T}_σ . If any of the edges of the quadrilateral lie on the $(n+2)$ -gon, then we consider the corresponding τ_i to be the empty word.

Proof. The theorem follows from the observation that each τ_i must contain at least one ear – a triangle of with edges $D_{i,i+1}, D_{i,i+2}, D_{i+1,i+2}$ – of the triangulation \mathcal{T}_σ . Therefore, under the clip sequence bijection, the word τ_i appears before τ_j if $i < j$. Moreover, the vertex labels j, k appear only after the two quadrants immediately adjacent to the vertex have been deleted under the clip sequence process. Thus, the two 312-avoiding permutations corresponding to the triangulation \mathcal{T}_σ and the triangulation resulting from applying an edge flip are precisely of the form described. \square

Example. Consider the permutation $\sigma = 154362$. If we wish to apply an edge flip to the diagonal $D_{2,6}$, then we can identify the vertex labels of the relevant quadrilateral as $i = 2, j = 3, k = 6$, and $l = 7$. This immediately tells us that τ_1 and τ_3 are both empty and τ_2 is the subword 54. Therefore, Theorem 5.2 above implies that we simply interchange j and k to get the resulting permutation $\mu(\sigma) = 154632$. See Figure 10 for the triangulations \mathcal{T}_σ and the triangulation resulting from the edge flip.

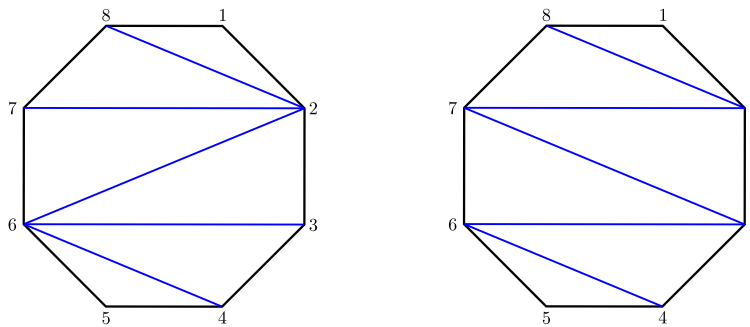


FIGURE 10. An edge flip at the diagonal $D_{2,6}$ in the triangulation \mathcal{T}_{154362} yields the permutation 154632.

Together with Theorem 5.1, the above computation gives an explicit combinatorial construction of Kalman loop in terms of geodesics paths of the flip graph and the corresponding behavior of 312-avoiding permutations.

REFERENCES

- [Ad90] V. I. Arnol’ d. *Singularities of caustics and wave fronts*, volume 62 of *Mathematics and its Applications (Soviet Series)*. Kluwer Academic Publishers Group, Dordrecht, 1990.
- [AdG01] V. I. Arnol’ d and A. B. Givental’. Symplectic geometry [MR0842908 (88b:58044)]. In *Dynamical systems, IV*, volume 4 of *Encyclopaedia Math. Sci.*, pages 1–138. Springer, Berlin, 2001.
- [ASS12] Ibrahim Assem, Ralf Schiffler, and Vasilisa Shramchenko. Cluster automorphisms. *Proc. Lond. Math. Soc.* (3), 104(6):1271–1302, 2012.
- [Cas21] Roger Casals. Lagrangian skeleta and plane curve singularities. *JFPTA*, Viterbo 60, 2021.
- [CG20] Roger Casals and Honghao Gao. Infinitely many Lagrangian fillings. arXiv:2001.01334, 2020.
- [CGGS20] Roger Casals, Eugene Gorsky, Mikhail Gorsky, and José Simental. Algebraic weaves and braid varieties. arXiv:2012.06931, 2020.
- [Che02] Yuri Chekanov. Differential algebra of Legendrian links. *Invent. Math.*, 150(3):441–483, 2002.
- [CN21] Roger Casals and Lenhard Ng. Braid loops with infinite monodromy on the legendrian contact dga. arXiv:2101.02318, 2021.
- [CZ21] Roger Casals and Eric Zaslow. Legendrian weaves. *Geom. Topol.*, 2021.
- [EHK16] Tobias Ekholm, Ko Honda, and Tamás Kálmán. Legendrian knots and exact Lagrangian cobordisms. *J. Eur. Math. Soc. (JEMS)*, 18(11):2627–2689, 2016.
- [EN19] John Etnyre and Lenhard Ng. Legendrian contact homology in \mathbb{R}^3 . <https://arxiv.org/pdf/1811.10966.pdf>, 2019.
- [Eul64] Leonhard Euler. Specimen algorithmi singularis. *Novi Commentarii academiae scientiarum Petropolitanae*, 9:53–69, 1764.
- [FOOO09] Kenji Fukaya, Yong-Geun Oh, Hiroshi Ohta, and Kaoru Ono. *Lagrangian intersection Floer theory: anomaly and obstruction. Part II*, volume 46 of *AMS/IP Studies in Advanced Mathematics*. American Mathematical Society, Providence, RI; International Press, Somerville, MA, 2009.
- [FWZ20a] Sergey Fomin, Lauren Williams, and Andrei Zelevinsky. Introduction to cluster algebras: Chapters 1-3. arXiv:1608.05735, 2020.
- [FWZ20b] Sergey Fomin, Lauren Williams, and Andrei Zelevinsky. Introduction to cluster algebras: Chapters 4-5. arXiv:1707.07190, 2020.
- [Gei08] Hansjörg Geiges. *An introduction to contact topology*, volume 109 of *Cambridge Studies in Advanced Mathematics*. Cambridge University Press, Cambridge, 2008.
- [GSW20] Honghao Gao, Linhui Shen, and Daping Weng. Augmentations, fillings, and clusters. arXiv:2008.10793, 2020.
- [Hug21] James Hughes. Weave realizability for d-type, 2021. <https://arxiv.org/abs/2101.10306>.
- [Kál05] Tamás Kálmán. Contact homology and one parameter families of Legendrian knots. *Geom. Topol.*, 9:2013–2078, 2005.
- [Kál06] Tamás Kálmán. Braid-positive Legendrian links. *Int. Math. Res. Not.*, pages Art ID 14874, 29, 2006.
- [Lev16] C. Levenson. Augmentations and rulings of Legendrian knots. *J. Symplectic Geom.*, 14(4):1089–1143, 2016.
- [Ng03] Lenhard L. Ng. Computable Legendrian invariants. *Topology*, 42(1):55–82, 2003.
- [Pan17] Yu Pan. Exact Lagrangian fillings of Legendrian $(2, n)$ torus links. *Pacific J. Math.*, 289(2):417–441, 2017.
- [Pou14] Lionel Pournin. The diameter of associahedra. *Adv. Math.*, 259:13–42, 2014.
- [Reg13] Alon Regev. A bijection between triangulations and 312-avoiding permutations. 2013.
- [STT88] Daniel D. Sleator, Robert E. Tarjan, and William P. Thurston. Rotation distance, triangulations, and hyperbolic geometry. *J. Amer. Math. Soc.*, 1(3):647–681, 1988.
- [STZ17] Vivek Shende, David Treumann, and Eric Zaslow. Legendrian knots and constructible sheaves. *Invent. Math.*, 207(3):1031–1133, 2017.
- [TZ18] David Treumann and Eric Zaslow. Cubic planar graphs and Legendrian surface theory. *Adv. Theor. Math. Phys.*, 22(5):1289–1345, 2018.
- [Ust06] A. V. Ustinov. A short proof of Euler’s identity for continuants. *Mat. Zametki*, 79(1):155–156, 2006.

UNIVERSITY OF CALIFORNIA DAVIS, DEPT. OF MATHEMATICS, SHIELDS AVENUE, DAVIS, CA 95616, USA

Email address: jmshughes@ucdavis.edu